FREEZE-DRYING AND REHYDRATION

Leonard Anderson Hamilton

NAVAL POSTGRADUATE SCHOOL
Monterey, California

THESIS

FREEZE-DRYING AND REHYDRATION

by

Leonard Anderson Hamilton

Thesis Advisor: P.F. Pucci

June 1973

Approved for public release; distribution unlimited.

Freeze-Drying and Rehydration

by

Leonard Anderson Hamilton
Lieutenant Commander, United States Navy
B.S., United States Naval Academy, 1961

Submitted in partial fulfillment of the
requirements for the degree of

MASTER OF SCIENCE IN MECHANICAL ENGINEERING

from the

NAVAL POSTGRADUATE SCHOOL

June 1973

ABSTRACT

Experimental results using roast turkey meat were obtained substantiating the uniformly retreating ice front model used in freeze-drying.

A one-dimensional model for rehydration was developed, based on flow in capillary tubes. Experimental results using roast turkey meat compared favorably with model prediction for an effective capillary diameter of 0.0010 cm. The results indicate a rapid rehydration following the model behavior predicted, followed by a much slower rate of rehydration. Maximum rehydration of the samples tested was to approximately two thirds of the original water content, eighty percent of which occurred during the first, rapid rehydration period.

The experiments also confirmed the model prediction of increased rehydration with increasing temperature.

TABLE OF CONTENTS

LIST OF FIGURES

SYMBOLS

D'	effective internal mass transfer coefficient	FT^2/HR
d	diameter	FT
g	acceleration of gravity	FT/SEC^2
ΔH_s	latent heat of sublimation for ice	BTU/LBM
h	external heat transfer coefficient	$BTU/HR-FT^2-°F$
h_1	height of water in capillary	FT
k	thermal conductivity of dried layer	BTU/HR-FT-°F
k_c	external mass transfer coefficient	FT/HR
L	thickness of slab being dried from both sides	FT
L_1	height of capillary	FT
ΔL	thickness of dried layer	FT
M	mass of substance = $M_d + M_w$	LBM
M_d	mass of freeze-dried substance	LBM
M_o	mass of original substance (before freeze-drying) = $M_d + M_{w_x}$	LBM
M_w	mass of water in substance	LBM
M_{w_x}	mass of water in original substance	LBM
$\mathcal{M}_w$	molecular weight of water	LBM/LBM-MOLE
N_A	molar flux of component A	$LB-MOLE/HR-FT^2$
p_{ew}	partial pressure of water vapor in equilibrium with the moisture sink	LBF/FT^2
p_{fw}	partial pressure of water vapor in equilibrium with the sublimation front	LBF/FT^2
p_{sw}	partial pressure of water vapor in equilibrium with the specimen surface	LBF/FT^2
q	heat flux	$BTU/HR-FT^2$
R	gas constant	FT-LBF/LBM-°R
R_H	rehydration number, = M/M_o	-

R_{HD}	rehydration number of freeze-dried substance, = M_d/M_o	-
r	fraction of rehydration, = M_w/M_{w_x}	-
T	temperature	°R
T_e	external temperature, temperature of heat source	°F
T_f	temperature of the sublimation front	°F
T_s	temperature of the outer surface of the specimen	°F
u_{AVG}	average velocity	FT/SEC
V_w	volume of fluid occupied by unit weight of water initially	FT^3/LBM
v_w	specific volume	FT^3/LBM
x	fraction of initial water present in substance	
γ	surface tension	LBM/SEC^2
θ	time since start of drying	HRS
μ	viscosity	LBM/FT-SEC
ρ	density	LBM/FT^3
ϕ	contact angle	RADIANS

ACKNOWLEGEMENT

Significant expertise in the field of freeze-drying was provided by Dr. C. Judson King; Chairman, Department of Chemical Engineering, University of California, Berkeley. The author had several consultations with Dr. King who provided a significant perspective on the current state of freeze-drying and gave meaningful counsel on fruitful areas of potential thesis effort. In addition, Dr. King provided the opportuntiy for the author to spend two afternoons in the University of California, Berkeley Freeze-Drying Laboratory observing the plant operation during freeze-drying evolutions and consulting with the plant operators who were Berkeley students engaged in Post-Doctoral-Studies Research for Dr. King.

The author wishes to express appreciation to the Library Staffs of both the Naval Postgraduate School and the University of California, Berkeley.

Miss Lyke is commended and thanked for her continued assistance in the areas of reference research and inter-library loan and for her consistently rapid procurement of essential periodical source material.

The author wishes to express appreciation to Ken Mothersell, Joe Beck, and Tom Christian, all of the Mechanical Engineering Department, for their assistance in the mechanical overhaul and electronic upgrading of the freeze-drying plant.

The nature of the work done on the plant also involved Bob Crompton and Ivan Gillis of Base Public Works and Bob Moeller of the Physics Department. Their timely, and enthusiastic response to "out of department" requests was quite gratifying. Because of their technical competence the plant overhaul and upgrading was successfully completed without the purchase of additional major components.

The author feels particularly privileged to have had Dr. Paul F. Pucci as Thesis Advisor. It was because of Dr. Pucci's interest and sponsorship that the freeze-drying plant was originally built. It was Dr. Pucci who suggested the utilization of the resources at Berkeley, thus significantly upgrading the quality of the research and consultation efforts. The author has realized, under the sponsorship and guidance of Dr. Pucci, a thesis effort which has been educational, fulfilling, and surprisingly enjoyable.

I. INTRODUCTION

Freeze-drying is a process in which the water frozen within a substance is removed by sublimation. In order to ensure that the water passes directly from a solid phase to a vapor phase without passing through a liquid phase the temperature of the substance is maintained below the triple point temperature of water (32.02°F or 491.69°R).

There are several advantages to dehydration through sublimation rather than through evaporation. In the field of food preservation freeze-drying is superior to every other drying method in producing the highest quality product. In contrast to the shrunken, shrivelled product of evaporation, the freeze-dried specimen essentially retains its previous size and cellular structure. This is because of the structural rigidity provided by the frozen state of the material. This porous, non-shrunken structure will easily and almost completely re-hydrate.

The low processing temperature involved in freeze-drying helps to minimize the extent of various degradative chemical reactions which often occur during drying processes such as non-enzymatic browning protein denaturation and enzymatic reaction [Ref. 1].

The relative absence of liquid water also helps to minimize degradative reactions and in addition prevents relocation of any soluble species during drying.

Another advantage of freeze-drying is that the local area undergoes a rapid transition from a completely hydrated to a nearly completely dehydrated condition. This also contributes to the minimizing of the degradative reactions already mentioned.

Freeze-drying has been used for the preservation of biological specimens for many years. Freeze-drying was used for the preservation of blood-plasma during World War II [Ref. 2]. At the present time the largest applications of freeze-drying are in the field of food preservation. Many other applications have been suggested and explored, including ... "the dehydration of radioactive wastes, the preparation of porous catalysts, the stabilization of free radicals, and the sublimation of non-aqueous solvents to allow operation in different media at different temperatures." [Ref. 1]. Noyes [Ref. 4] provides a summary of the progress and developments in freeze-drying by many organizations and corporations in several countries.

Freeze-drying has been described in general in works by Cotson and Smith [Ref. 5], Rey [Ref. 3] and Van Arsdel [Ref. 6]. Comprehensive reviews were published by Harper and Tappel [Ref. 7] in 1957 and by Burke and Decaureau [Ref. 8] in 1964. In 1963 the United States Department of Agriculture published a list of 638 freeze-drying references which had been published prior to 1963 [Ref. 9]. A summary of the work on the drying of solids in the Soviet Union was published by Fulford [Ref. 10] in 1969.

II. PHYSICAL MECHANISM OF FREEZE-DRYING

An analytical evaluation of the mechanism of freeze-drying is beneficial from the viewpoint of determining the parameters that affect freeze-drying rates and how changes in these pertinent parameters result in changes in the rates. These considerations are important because of the requirements of both science and industry to provide an economical, consistent, high-quality product.

A. NATURE OF THE FROZEN FRONT

Most qualitative analyses of the mechanism of freeze-drying have assumed that a discrete surface divides the frozen hydrated region from the dehydrated region. The assumption is that initially a very thin layer at the surface nearly completely sublimates and that the frozen front then moves inward, leaving a dehydrated solid material. This idealization had been universally assumed and accepted. Recently, however, discussion has occurred challenging the validity of this assumption.

1. Arguments Against a Sharp Frozen Front

Meffert [Ref. 11] concluded that a significant percentage of the initial water content was not removed by the frozen front, but was left behind and finally removed by secondary desorption.

Bralsford [Ref. 12] inferred that if any liquid were present a liquid diffusion effect could exist. He

concluded that this might undermine the validity of the sharp frozen front model.

Brajnikov et al. [Ref. 13] performed several elaborate experiments and concluded that a transition zone existed in the sublimation front.

Luikov [Ref. 14] reports in great detail the behavior of a sublimation front. These studies can account for a transition zone of, at the most, one millimeter in thickness.

In each of the experiments previously cited there were undermining physical factors that precluded the definitive conclusion of a diffuse sublimation front. In several experiments sample layer thickness and thermocouple thickness were of the same order of magnitude as the thickness of the reported transition zone. In other cases melting occurred, because of improper temperature control or due to the presence of artifical salts which had been introduced for experimental purposes.

2. Arguments For a Sharp Frozen Front

Many studies relate the physical visual observation of a sharp discrete frozen front separating the frozen fully hydrated portion of the sample from the almost fully dehydrated uniformly discolored portion. This was observed and reported by Harding [Ref. 15] in beef, Margaritis and King [Ref. 16] in turkey meat and Beke [Ref. 17] in pork.

In addition to physically observing this phenomenon Beke shows photographs which reveal a distinct frozen front separating the dry zone from the darker frozen zone. Photographs are also provided by Clark [Ref. 18]. These also show a sharp demarkation between the frozen and dehydrated regions of the specimen.

Hatcher [Ref. 19] used gamma ray attenuation to measure the moisture profile across his sample. Visual inspection revealed a planar ice-front. In addition the ice front was observed to be sharper than the 3/16 inch diameter of the gamma ray beam. The gamma ray count indicated no residual moisture once the sublimation front had passed. Of particular interest are Hatcher's reports of temperature histories during the freeze-drying of beef slabs. Measurements were made with thermocouples embedded in the body of the samples. Figure 1 is a plot of temperatures versus time for various thermocouple positions. Figure 2 is a plot of the same temperatures versus thermocouple distance from the sample surface for various times. From these plots it is observed that a sharp transition occurs from the frozen zone of uniform low temperature to the dry zone with a nearly linear temperature gradient.

Similar results have been observed by Speiss [Ref. 20] in the freeze-drying of potato starch and egg white and by Sandall et al. [Ref. 21] in the freeze-drying of turkey meat.

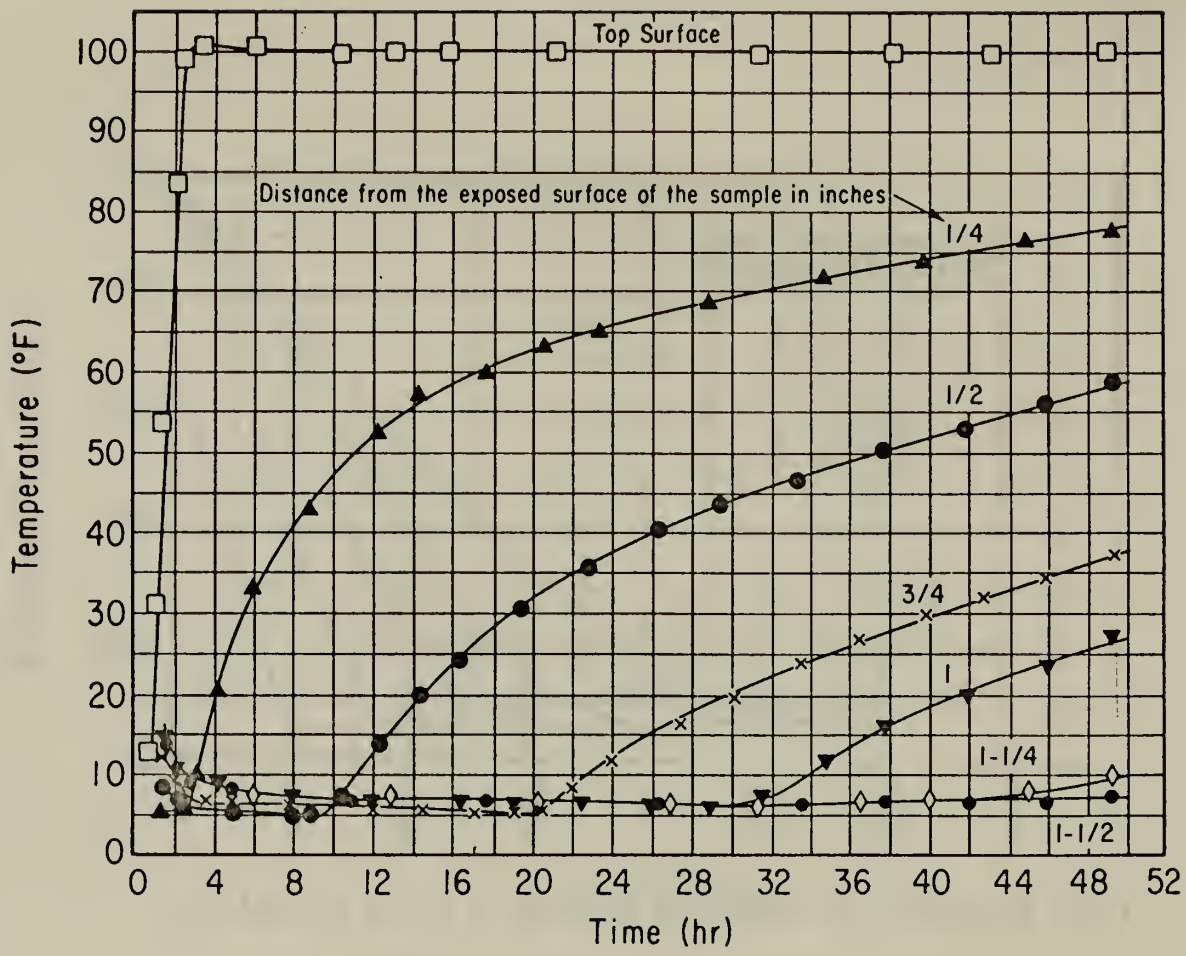

Figure 1. Temperature versus time at different thermocouple locations during the freeze-drying of beef. Hatcher [Ref. 19].

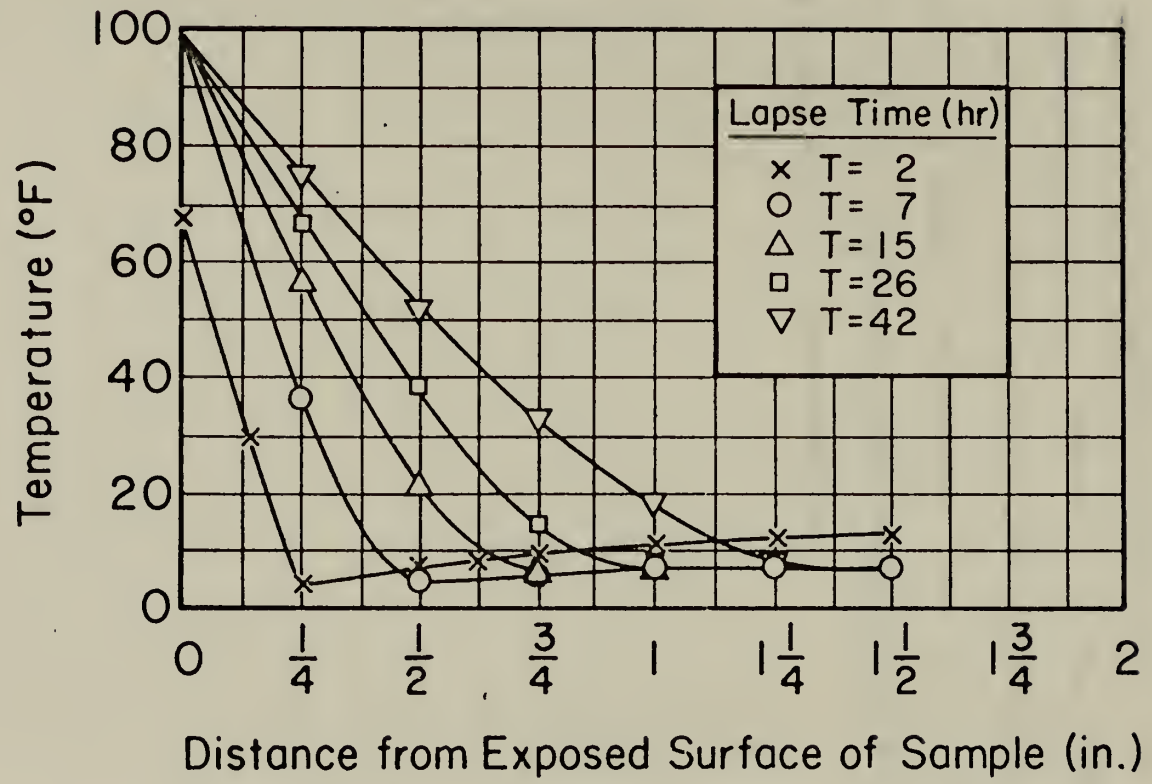

Figure 2. Temperature versus position at different times during the freeze-drying of beef. Hatcher [Ref. 19].

B. CONCLUSIONS

King [Ref. 1] concludes that there are factors such as structural irregularities and molecular and crystallitic phenomenon which may cause a diffuse sublimation front. He points out, however, that they operate over short distances. It is acknowledged that, as the temperature inside the material approaches the melting temperature, the frozen front will become more diffuse. However, in the temperature ranges which result in a high-quality freeze-dried product the supposition of a sharp sublimation front is valid and in fact more accurate than many other assumptions made in the design and analysis of freeze-drying.

III. THEORY OF FREEZE-DRYING

Figure 3 [Ref. 1] shows the several factors which interact to govern the freeze-drying rates. A heat source is necessary to provide the heat of sublimation of 1200 BTU per pound of water. A moisture sink is required to remove the generated water vapor. The driving force for the heat transfer is the temperature difference between the heat source and the sublimation front. The driving force for the mass transfer is the partial pressure difference between the partial pressure of the water vapor in equilibrium with the sublimation front and the partial pressure of water vapor in equilibrium with the moisture sink.

A. THE FREEZE-DRYING MODEL

The model most often used in an analytical study of freeze-drying is the Uniformly Retreating Ice Front Model (URIF) shown in Figure 4 [Ref. 22]. It is assumed that the heat ransfer and the mass transfer occur at a pseudo steady-state across the dry layer. It is further assumed that the linear temperature profile across the dry surface is not distorted by the outflow of water vapor. Sandall [Ref. 21] and Sandall and others [Ref. 22] made theoretical studies of these assumptions and determined that the maximum error introduced by either of these assumptions was four percent of the predicted rate of heat or mass transfer. Finally it is assumed that complete drying occurs during the retreat of the sublimation front. Sandall and others

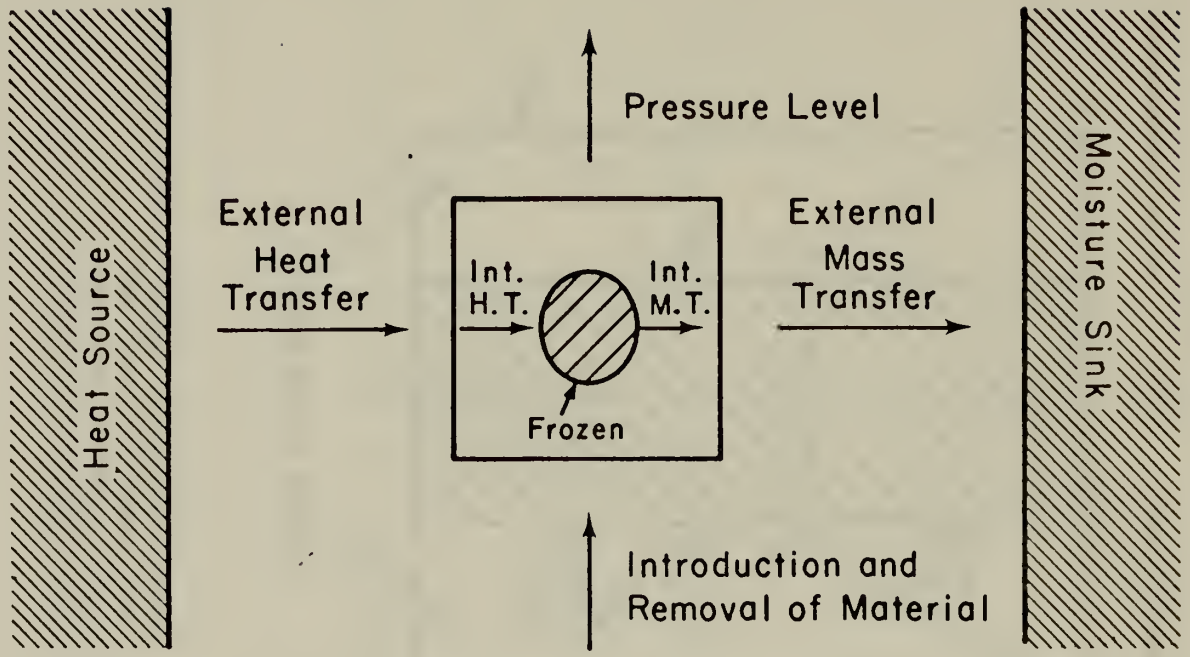

Figure 3. Factors influencing rates of freeze-drying. King [Ref. 1].

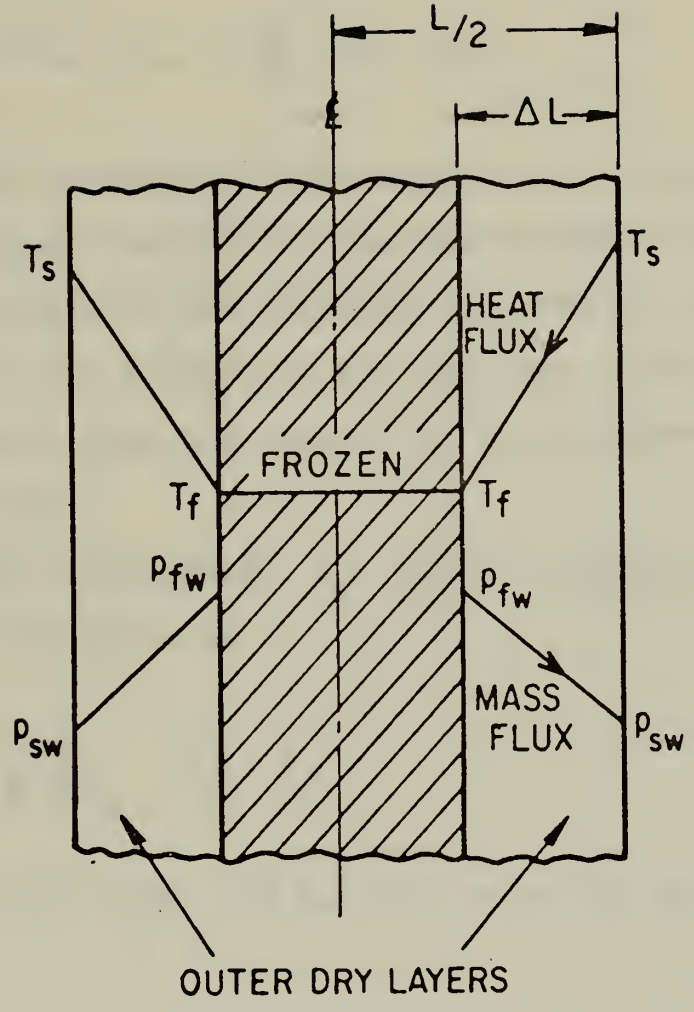

Figure 4. Model of a uniformly retreating ice front for the freeze-drying process. King [Ref. 1].

[Ref. 22] determined that a maximum error of three percent resulted from this assumption.

For these conditions, the expression for heat transfer is [Ref. 22]

$$q = h(T_e - T_s) = \frac{k}{\Delta L}(T_s - T_f) \tag{1}$$

where the heat transfer to the substance by convection is equal to the heat transfer through the substance by conduction. The convection heat transfer is from the external heat source to the surface of the specimen. The conduction heat transfer is from the surface of the specimen to the sublimation front.

The surface temperature, T_s, can be eliminated from Equation (1) resulting in

$$q = \frac{k}{\frac{k}{h} + \Delta L}(T_e - T_f) \tag{2}$$

Similarly the mass flux has the following expression [Ref. 22]

$$N_{A_w} = \frac{k_c}{R\bar{T}}(p_{sw} - p_{ew}) = \frac{D'}{R\bar{T}}\frac{p_{fw} - p_{sw}}{\Delta L} \tag{3}$$

where the mass transfer external to the specimen is equal to the mass transfer internal to the specimen. The mass transfer internal to the specimen is from the sublimation

front to the specimen surface. The mass transfer external to the specimen is from the specimen surface to the moisture sink.

Note that $\bar{T}$ is the average of the absolute temperature of the specimen surface and the frozen surface. The assumption that $\bar{T}$ is constant will result in no more than two percent error using the extremes of temperatures experienced in this experiment.

The surface partial pressure can be eliminated from Equation (3), resulting in

$$N_A M_w = \frac{D'}{\frac{D'}{k_c} + \Delta L} \frac{1}{R\bar{T}} (p_{fw} - p_{ew}) \qquad (4)$$

Since it is assumed that complete drying occurs behind the sublimation front, the fraction of water remaining in the substance, x, is equal to the fraction of the substance still frozen. Thus:

$$x = \frac{\frac{L}{2} - \Delta L}{\frac{L}{2}}$$

Solving for ΔL yields

$$\Delta L = \frac{L}{2} (1 - x) \qquad (5)$$

Substituting Equation (5) into Equation (2) yields

$$q = \frac{k}{\frac{k}{h} + (1-x)\frac{L}{2}} (T_e - T_f) \tag{6}$$

Substituting Equation (5) into Equation (4) yields

$$N_A \mathcal{M}_w = \frac{D'}{\frac{D'}{k_c} + (1-x)\frac{L}{2}} \frac{(p_{fw} - p_{ew})}{R\bar{T}} \tag{7}$$

Assuming that the temperatures in the specimen are not changing rapidly it follows that

$$q = \Delta H_s \mathcal{M}_w N_A \tag{8}$$

where the heat flux from the specimen is equal to the product of the molar flux times the molecular weight times the latent heat of sublimation.

Multiplying Equation (7) by $H_s \mathcal{M}_w$ and dividing Equation (7) by Equation (6) yields

$$\frac{p_{fw} - p_{ew}}{T_e - T_f} = \frac{k}{D'} \frac{R\bar{T}}{\mathcal{M}_w} \frac{1}{\Delta H_s} \left\{ \frac{\frac{D'}{k_c} + (1-x)\frac{L}{2}}{\frac{k}{h} + (1-x)\frac{L}{2}} \right\} \tag{9}$$

This is known as the "wet-bulb" relationship for freeze-drying [Ref. 22].

Evaluating this "wet-bulb" relationship for conditions at the surface of the sample leads to [Ref. 21]

$$\frac{p_{fw} - p_{sw}}{T_s - T_f} = \frac{k}{D'} \frac{R\bar{T}}{M_w} \frac{1}{\Delta H_s} \tag{10}$$

From Equation (10) it is concluded that fixing T_s and therefore p_{sw}, results in a decreasing p_{fw} with an increasing T_f. However, at saturation the partial pressure increases with increasing temperatures. Thus, the temperature and partial pressure must remain constant to satisfy Equation (10) and the natural phenomenon involved.

Applying a similar argument to Equation (9) it is concluded that a constant T_s and p_{sw} will also exist for a constant T_e and p_{ew} if h and k_c are sufficiently large when compared to the internal coefficients.

The drying rate can then be related to the heat and mass transfer rate equations [Ref. 22].

Heat:

$$\frac{L}{2} \frac{\Delta H_s}{V_w} \left(-\frac{dx}{d\theta}\right) = \left\{ \frac{k}{\frac{k}{h} + (1-x)\frac{L}{2}} \right\} (T_e - T_f) \tag{11}$$

Mass:

$$\frac{L}{2} \frac{1}{V_w} \left(-\frac{dx}{d\theta}\right) = \left\{ \frac{D'}{\frac{D'}{k_c} + (1-x)\frac{L}{2}} \right\} \frac{M_w}{R\bar{T}} (p_{fw} - p_{ew}) \tag{12}$$

These equations, (11) and (12), can now be rearranged into forms more useful for testing the validity of this model and for attaining the transport coefficients from drying rate data [Ref. 22]

$$(1-x) = \frac{4kV_w}{\Delta H_s L^2} \left\{ \frac{T_e - T_f}{(-\frac{dx}{d\theta})} \right\} - \frac{2}{L} \frac{k}{h} \qquad (13)$$

and

$$(1-x) = \frac{4D'V_w M_w}{L^2 R\bar{T}} \left\{ \frac{p_{fw} - p_{ew}}{(-\frac{dx}{d\theta})} \right\} - \frac{2}{L} \frac{D'}{k_c} \qquad (14)$$

Thus it is anticipated that a plot of (1-x) versus $\left\{ \frac{T_e - T_f}{(-\frac{dx}{d\theta})} \right\}$ would be linear with the slope dependent on the thermal conductivity and the intercept dependent on the external heat transfer.

Similarly, a plot of (1-x) versus $\left\{ \frac{p_{fw} - p_{ew}}{(-\frac{dx}{d\theta})} \right\}$ should be linear with the slope dependent on the internal mass transfer coefficient and the intercept dependent on the external mass transfer coefficient. Because of the two variables in the second term of Equations (13) and (14) it is necessary to solve for the slope first, solve for k and D' respectively, then evaluate the intercept and solve for h and k_c with k and D' already known.

In addition to the assumptions and simplifications noted in Section III.A. it is assumed that internal energy absorbed by the dry layer to increase its temperature as freeze-drying progresses is negligible. Sandall [Ref. 21] evaluated this

assumption and found that the maximum error for the most extreme conditions of freeze-drying was four percent.

Similarly it is concluded that the energy required to heat the vapor as it flows through the dry layer is negligible.

B. TRANSPORT PROPERTIES

1. Thermal Conductivity

Figure 5 [Ref. 21] is a plot of the thermal conductivity of freeze-dried turkey meat versus pressure. These measurements were made in a steady heat flux, thermopile apparatus. At very low pressure where the mean free path of the vapor is much greater than the pore diameter of the specimen it is observed that the vapor provides no significant contribution to the overall thermal conductivity. As pressure increases the mean free path of the vapor decreases until it is on the order of magnitude of the pore diameter. Continued increase in pressure results in a linear decrease in the mean free path and a linear increase in thermal conductivity. At high pressures the mean free path of the vapor is very small compared to pore diameter and the effective thermal conductivity does not vary with pressure.

2. Mass Transfer

Figure 6 [Ref. 21] is a plot of the internal mass transfer coefficient of turkey meat versus total pressure. The average Knudsen and Bulk Diffusion coefficients of

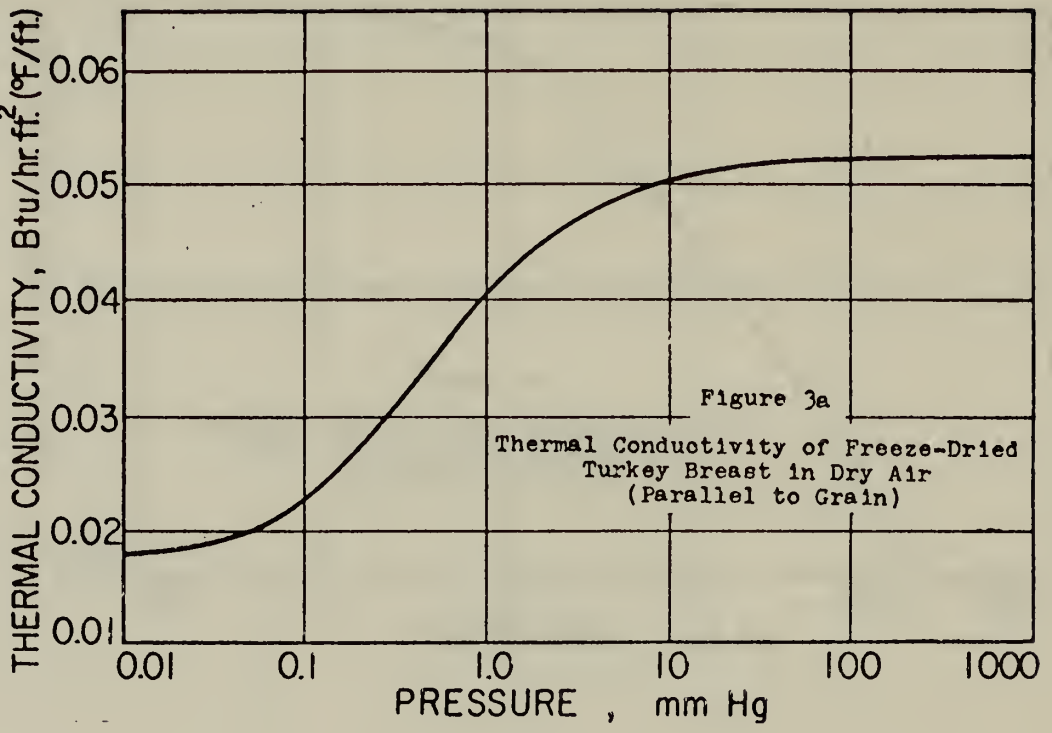

Figure 5. Thermal conductivities of freeze-dried turkey breast in dry air, Sandall and others [Ref. 22]

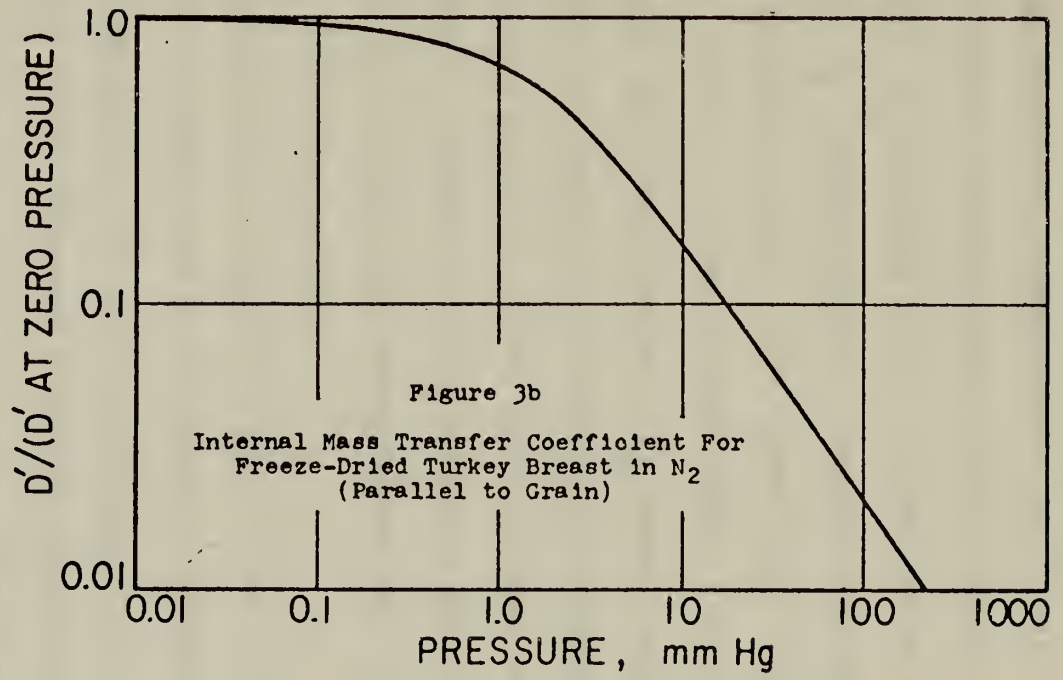

Figure 6. Internal mass transfer coefficient for freeze dried turkey breast in N_2. Sandall [Ref. 21].

turkey meat were measured by Gunn [Ref. 22] and plotted. It is observed that at the lower pressures the flux is maximum. As pressure decreases, the mean free path of the vapor increases with the result that the flux varies inversely with pressure.

C. THE LIMITS

It is necessary to acknowledge that limits exist for both the heat transfer driving force and the mass transfer driving force. There is an upper limit to the outer surface temperature, T_s, beyond which, thermal degradation of the dried product will occur. The upper limit for most meats is about 60°C. [Ref. 6]. The second limit is the upper limit to the frozen zone temperature, T_f, above which the undried portion would no longer be frozen. Of interest, this is not the melting point of water but normally several degrees lower. Sandall, [Ref. 21] for example, found that for turkey meat the maximum ice temperature was -5°C, primarily because of dissolved solids.

It is observed in Figures 5 and 6 that at very low pressures k is small and D' is large. Applying these factors to Equation (10) and increasing T_s to increase the drying rate, it is observed that the outer surface temperature, T_s, will reach its limit before the ice temperature, T_f. Thus the drying rate is more effectively increased by increasing k than by increasing D'. Thus freeze-drying at low pressure is heat-transfer controlled.

Again from Figures 5 and 6 it is observed that at relatively high pressures, k is large and D' is small. Applying to Equation (10) and increasing T_s to increase the drying rate, it is observed that the ice temperature, T_f, will reach its limit before the outer surface temperature T_s. Thus the drying rate is more effectively increased by increasing D' than by increasing k. Thus high pressure freeze-drying is mass-transfer controlled.

IV. THEORY OF REHYDRATION

Relatively little study or research has been undertaken in the area of rehydration of freeze-dried foods.

King, Lam and Sandall [Ref. 24] determined that conditions which resulted in a lack of shrinkage during the freeze-drying of turkey also resulted in improved rehydration. These findings were confirmed by Beke [Ref. 17] as also applicable to pork.

Karel[Ref. 25] observed a decrease in the rehydration of haddock fillets freeze-dried with an increase in the frozen zone and outer surface temperatures. Karel also observed that for freeze-dried salmon the obverse was true; improved rehydration occurred for samples processed with higher frozen zone and outer surface temperatures.

Goldblith [Ref. 3] determined that for freeze-dried shrimp higher frozen zones and outer surface temperatures resulted in reduced rehydration.

Karel [Ref. 25], Goldblith [Ref. 3] and Cotson and Smith [Ref. 5] observed that raw meat and fish were much superior in quality when rehydrated with cold water than with hot water over a range from 40°F to 212°F. The samples rehydrated with hot water had a tough fibrous texture and a "twice-cooked" flavor. This result was thought to be because of the protein denaturation resulting from the higher rehydration temperatures.

Hamm [Ref. 26] also observed the decrease in the water holding capacity of freeze-dried beef with increasing rehydration water temperature and observed that a significant decrease in rehydration began at 86°C.

A. THE REHYDRATION MODEL

Margaritis and King [Ref. 16] developed a structural model of a single fiber based on their microscopic measurements and supplemented by histological information given by Maximow and Bloom [Ref. 27]. This model is illustrated in Figure 7.

The wet fiber is contained by the cell wall, the sarcolemma, a membrane of one micron thickness. The fiber is made up of myofibrils one micron in diameter with a one-tenth micron separation distance. The fiber itself has a diameter of 36 microns. In the unfrozen state the myofibrils are distributed evenly throughout the fiber, Figure 7(a).

During freezing the water moves to the center of the fiber, forming an ice core and forcing the myofibrils toward the sarcolemma.

When frozen the fiber has a single ice column of 24 microns diameter at the center of the column. The myofibrils are shrunken and closely packed into the 5 micron annulus lying between the sarcolemma and ice core, Figure 7(b).

The freeze-dried fiber has the same dimensions as the

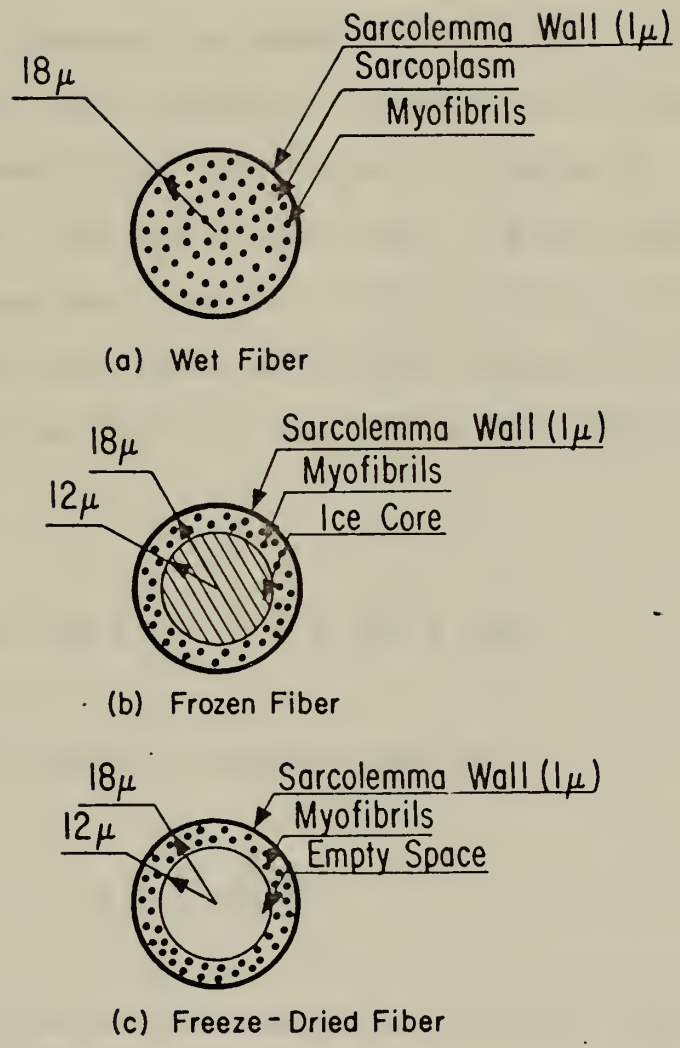

Figure 7. Cross-section of a model fiber. Margaritis and King [Ref. 16].

frozen fiber with the ice column removed from the center of the fiber, Figure 7(c).

Koonz and Ramsbottom [Ref. 28] studied the formation of crystals in poultry tissue using a wide variety of freezing rates. Their conclusions verify the validity of this model of a single ice column in each fiber.

B. CAPILLARITY AND SURFACE TENSION

The above rehydration model consisting of a single ice column in each fiber suggests a model involving capillarity and surface tension as illustrated in Figure 8.

Moore [Ref. 29] and Barrow [Ref. 30] developed the equation for surface tension. This involves a static balance between the force of surface tension in the upward direction and the force of gravity in the downward direction.

$$\pi d\gamma \cos \phi = \left(\frac{\pi d^2}{4} \right) \rho g h_1 \qquad (18)$$

Solving for surface tension yields

$$\gamma = \frac{d}{4} \frac{\rho g h_1}{\cos \phi} \qquad (19)$$

For water the contact angle, ϕ, is zero [Ref. 29] resulting in

$$\gamma = \frac{d}{4} \rho \, g \, h_1 \qquad (20)$$

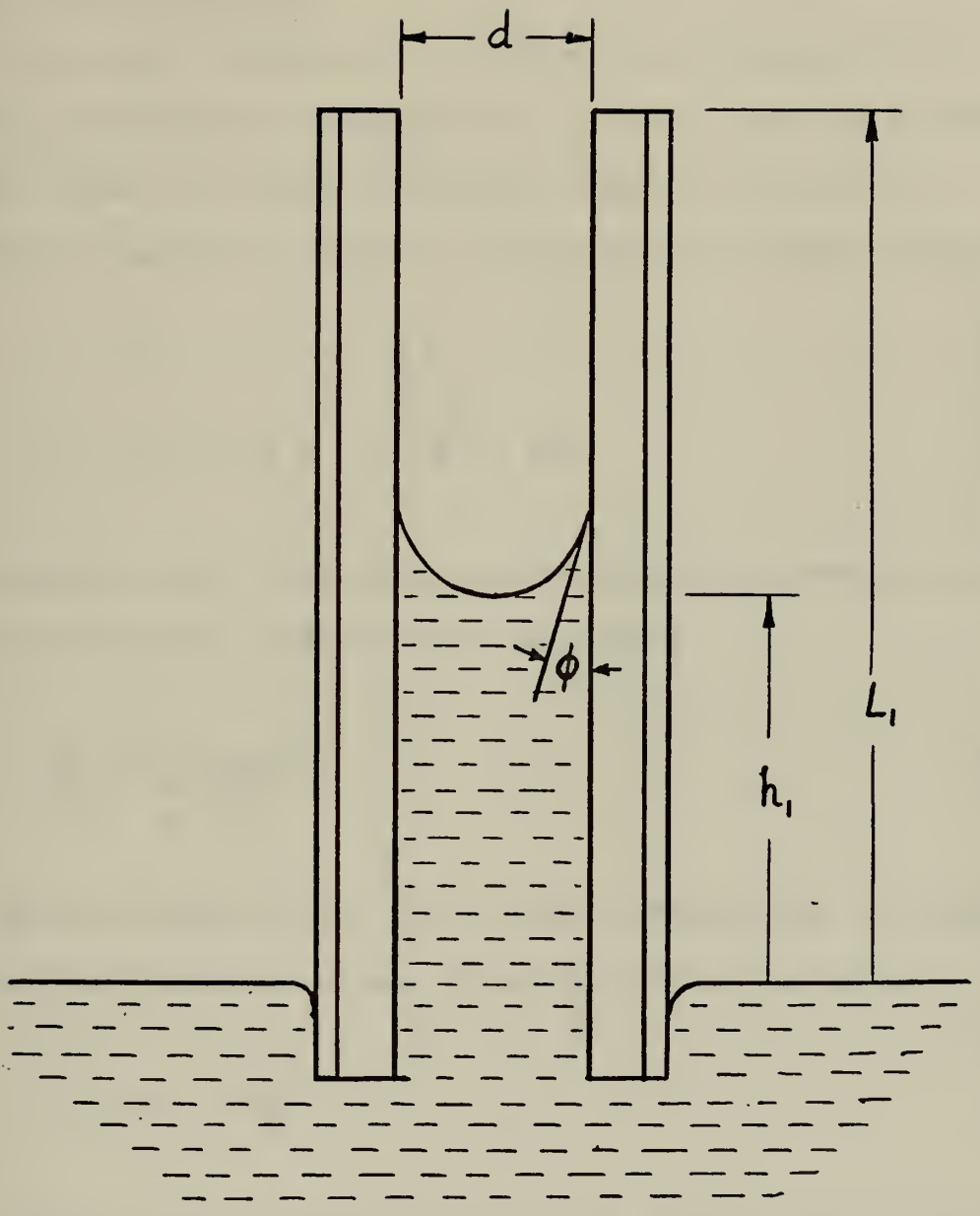

FIGURE 8. Capillary Model

Equation (20) is an expression for surface tension under steady state conditions which will describe the ultimate degree of rehydration.

It is also desirable to formulate an expression describing the rate of rehydration. In this case the difference of the terms for force of surface tension and force of gravity is taken in order to obtain the net upward force, F_z.

$$F_z = \pi d\gamma \cos \phi - \left(\frac{\pi d^2}{4} \right) \rho g h_t \tag{21}$$

Streeter [Ref. 31] gives the following expression for pressure drop for laminar flow in a pipe

$$\frac{\Delta P}{h_t} = \frac{32\ u_{AVG}\ \mu}{g_c\ d^2} \tag{22}$$

The net upward force due to the differential pressure is that differential pressure multiplied by the area

$$F_z = \Delta P \left(\frac{\pi d^2}{4} \right) \tag{23}$$

Combining Equations (22) and (23) yields the following expression for F_z

$$F_z = \frac{8\pi\ u_{AVG}\ \mu\ h_t}{g_c} \tag{24}$$

And combining Equations (21) and (24) yields

$$\frac{8\pi\, u_{AVG}\, \mu\, h_1}{g_c} = \pi\, d\gamma\, \cos\phi - \left(\frac{\pi d^2}{4}\right)\rho g h_1 \quad (25)$$

Solving Equation (25) for average velocity yields

$$u_{AVG} = \frac{dh_1}{dt} = \frac{\left[\pi d\gamma \cos\phi - \left(\frac{\pi d^2}{4}\right)\rho g h_1\right]}{\frac{8\pi h_1 \mu}{g_c}} \quad (26)$$

An order of magnitude comparison of the two terms in the numerator of Equation (26) indicates that the magnitude of the second term is always less than two percent of the first term for the samples used in this experiment.

Thus Equation (26) now becomes

$$u_{AVG} = \frac{dh_1}{dt} = \frac{d\gamma g_c}{8h_1\mu} \quad (27)$$

Rearranging and integrating yields

$$\int_0^{h_1} h_1\, dh_1 = \frac{d\gamma g_c}{8\mu} \int_0^{t} dt \quad (28)$$

$$h_1^2 = \frac{d\gamma g_c t}{4\mu} \quad (29)$$

Recall that Equation (29) resulted from the development of a vertical capillary model in which the force of gravity

acting against the capillary flow was negligible. This means that Equation (29) is valid for a horizontal capillary model if the force of gravity acting in the direction of capillary flow is also negligible. Numerical evaluation further indicates that this assumption is valid for specimens used in this experiment if rehydration immersion depths are not greater than three times the specimen dimension in the direction of the capillary.

Thus this dynamic analysis indicates that a second order response is expected. Specifically rehydration varies directly with the square root of capillary diameter, surface tension and time and inversely with the square root of viscosity.

Furthermore, this analysis indicates that for a given group of similar samples of constant diameter, rehydrated for the same period of time, the rehydration would vary with the square root of the ratio of surface tension over viscosity. Since this ratio increases with temperature, (Appendix B) it is qualitatively predicted that on the basis of temperature change alone, that rehydration increases with an increase in temperature.

V. EXPERIMENTAL RESULTS

Experimental rsults were undertaken with several objectives. It was desired to experimentally verify or refute: the concept of a discrete sublimation front; the freeze-drying model and the rehydration model. Furthermore it was desired to experimentally evaluate the effect of the varying of several parameters on the resulting rehydration.

A. GENERAL DESCRIPTION OF SYSTEMS

1. Vacuum System

Figure 9 illustrates the Vacuum System.

The vacuum is maintained by a National Research Corporation 100 S Rotary Gas Ballast Pump. The five horse-power pump has a capacity of 100 cubic feet per minute and a blank off pressure of ten to fifteen microns.

The main vacuum chamber is a modified National Research Corporation Model 2555 furnace tank. It is a 40 inch long by 40 inch diameter stainless steel cylinder. Access is through a door at one end of the cylinder. The door is moved by an air-controlled hydraulically-operated hoist. The door contains a viewing port. At the opposite end of the chamber is a variac controlled light. In the event of electrical failure, the main vacuum chamber is isolated by the automatic closing of the electrically-controlled air-operated high vacuum valve.

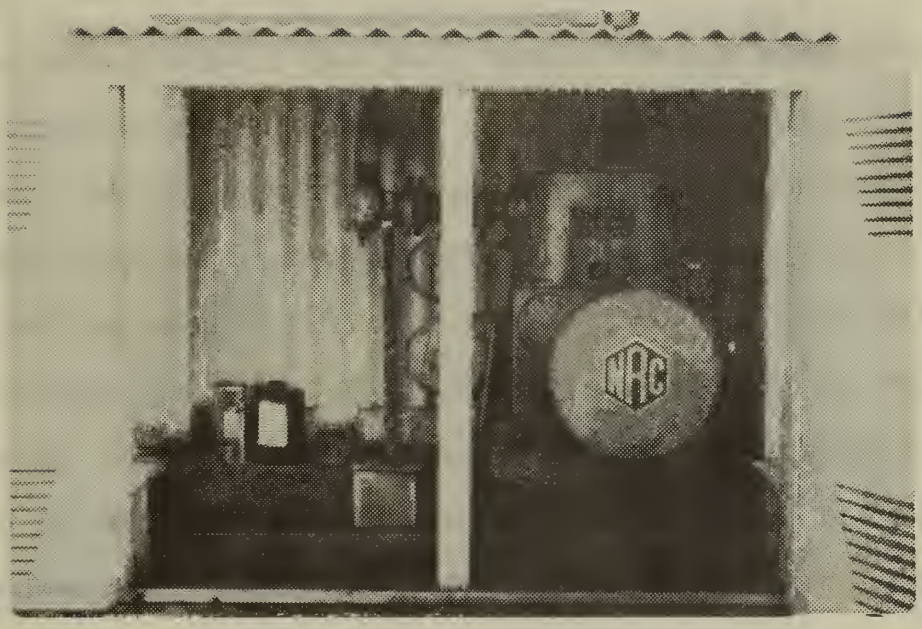

Figure 9. Vacuum System

The rotary gas ballast pump removes from the main vacuum chamber all non-condensible gases that enter the chamber when it is open to the atmosphere. In addition, the pump removes condensible gases that enter the chamber and also those that sublimate from the sample specimens. The pump discharges the non-condensible gases to the atmosphere. However the condensible gases, which are taken into the pump as vapors, condense during the compression portion of the pump cycle. These condensed gases contaminate the seal oil and reduce the pump efficiency and the quality of the vacuum. These condensible vapors are removed by the process of gas-ballasting. Gas-ballasting admits filtered air to the pump when the vacuum chamber is isolated by the rotating vane but before compression begins. Air and vapor are then compressed together to reach or exceed atmospheric pressure before the components of vapor individually reach the pressure at which they would condense.

2. Refrigeration System

Figure 10 illustrates the refrigeration system.

The main chamber is cooled by a one-third horsepower Tecumseh Products Company refrigeration plant charged with Freon 502. The refrigerant cools the main vacuum chamber by passing through stainless steel coils located in a 36" diameter cylindrical shell inside the chamber.

A condenser is attached to the main vacuum chamber. The condenser is cooled by a one-quarter horsepower Bendix-

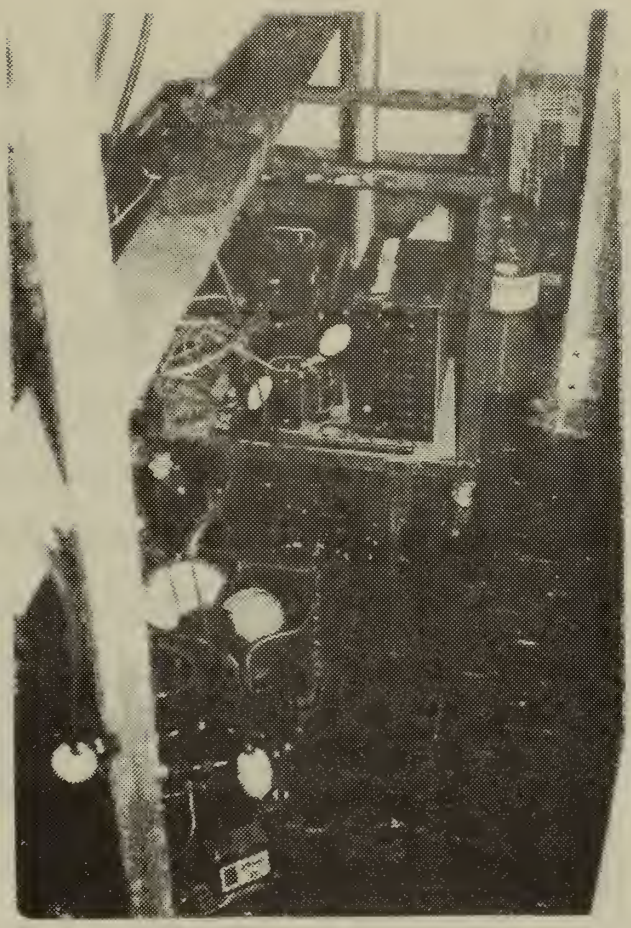

Figure 10. Refrigeration System

Westinghouse Corporation refrigeration plant charged with Freon 502. The refrigerant cools the condenser by passing through three sets of concentric copper coils.

3. Electrical System

All power provided to the freeze-drying plant is 110 volt, 60 cycle A.C.

In addition to the electrical components already mentioned there is an electrically-controlled air-operated foreline valve. This valve closes automatically on loss of electrical power.

4. Electronic System

Figure 11 illustrates the electronics system.

Pressure indication is provided by a Veeco Instruments, Incorporated, Thermocouple Gauge Control.

Temperature indication is provided by a Leeds and Northrup millivolt potentiometer.

Figure 12 illustrates the electronics associated with the weight change indication device (WCID). The WCID consists of the specimen tray suspended by a linear spring. The bottom of the tray is attached to the movable core of a linear core transducer. The transducer is excited by an audio oscillator. The transducer output is read on a Hewlett-Packard 3400 A voltmeter and a Mosely Autograf Model 7100 B strip chart recorder.

For a detailed description of the weight-change-indication device see Appendix C.

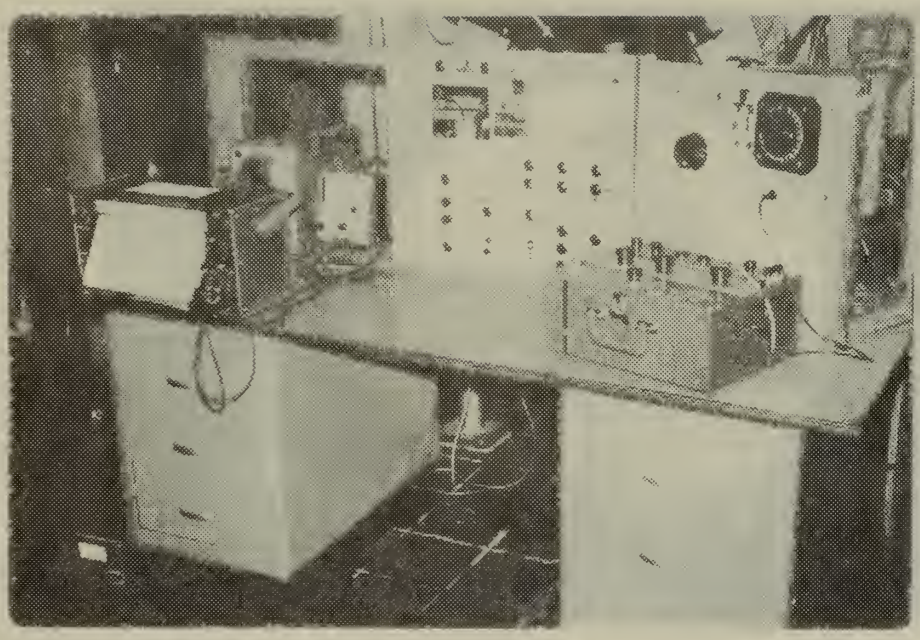

Figure 11. Electronic System

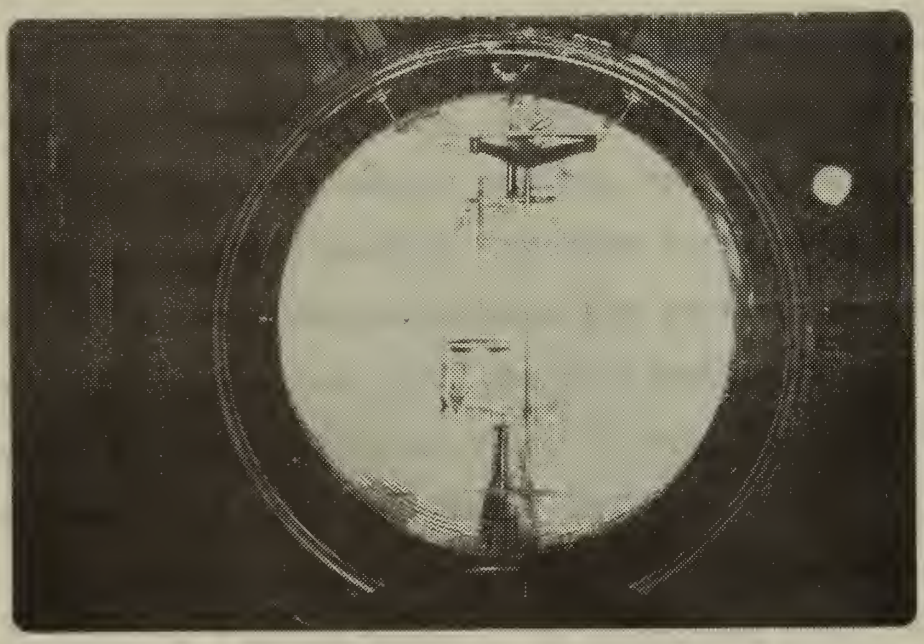

Figure 12. Weight Change Indication Device

5. System Operation

Prior to an actual freeze-drying evolution, all system components are operated until temperatures and pressures are at equilibrium.

The system is capable of maintaining a vacuum of 250 microns, a chamber temperature of -15°C and a condenser temperature of -30°C.

Next the frozen specimen which is at approximately -25°C is placed in the chamber and freeze-drying commences. The temperature difference driving force is the temperature difference between the heat source and the surface of the specimen. The water vapor partial pressure difference driving force is the difference between the partial pressure of water vapor in equilibrium with the sublimation front and the partial pressure of water vapor in equilibrium with the moisture sink. In this experiment the heat source is the inside chamber walls which are heated by the atmosphere. The moisture sink is the condenser. As discussed previously, the vacuum pump is capable of removing water vapor from the system. However, the primary purpose of the vacuum pump is to decrease the chamber pressure. This causes an increase in the mean free path of the vapor. As discussed in Section III.B.2 this results in an increased mass flow rate.

Figure 13 illustrates the inter-relationship of the various systems.

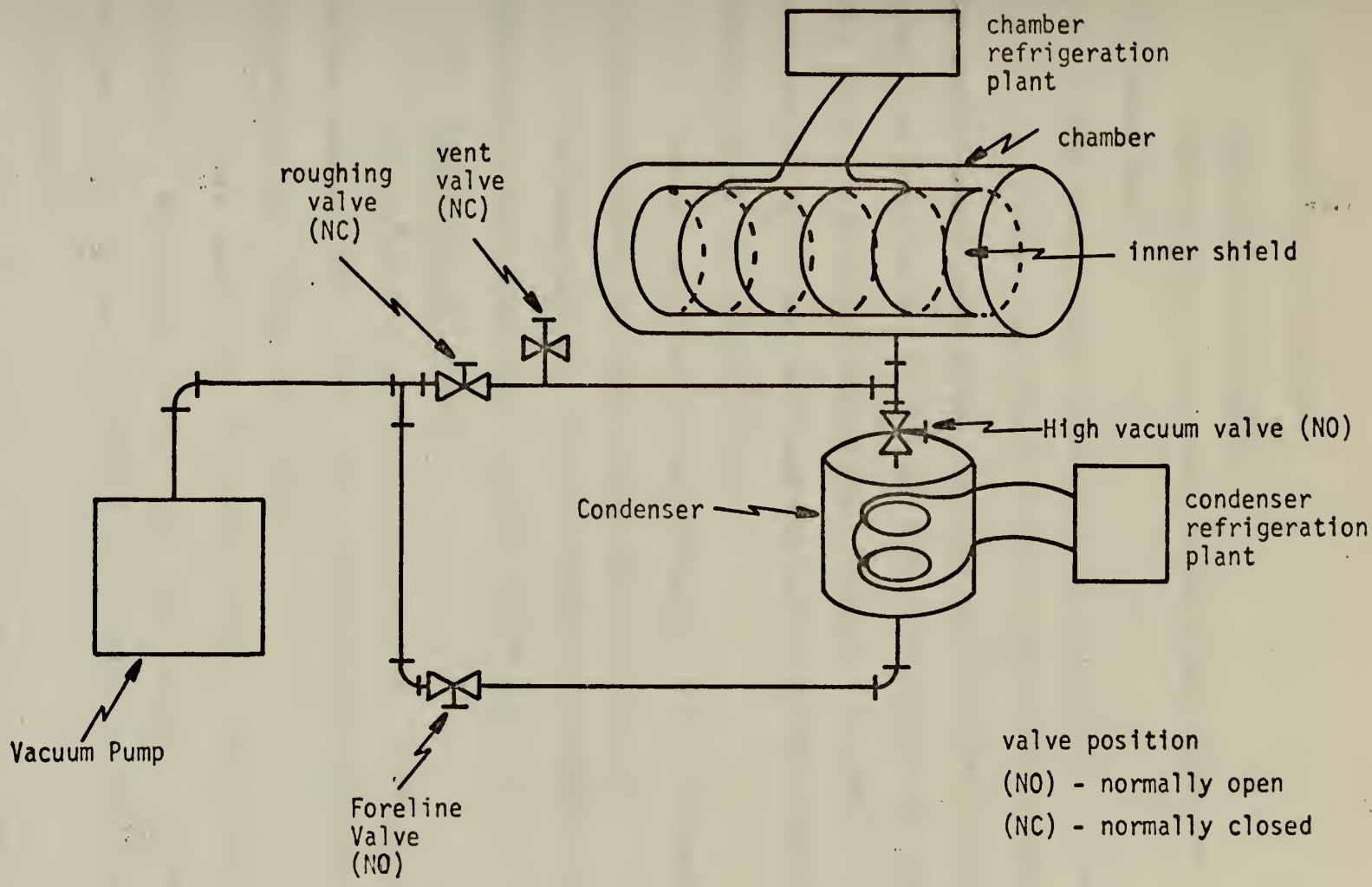

Figure 13. Freeze-Drying Plant

B. EXPERIMENTAL PROCEDURE

1. Preparation of Sample

Turkey breast meat was the specimen selected for this experiment.

The turkey was cooked for 110 minutes at 400°F.

The turkey was then cut into sample size pieces. Two sample sizes were used. Turkey roast slices, approximately one centimeter thick and ten centimeters in diameter were used for the one-dimensional studies (discrete sublimation-front analysis and evaluation of the models for freeze drying and rehydration).

Turkey roast cubes approximately two centimeters on a side were used for other rehydration studies.

The samples were then frozen in a freezer in which temperature was maintained between -25°F and -15°F.

2. Processing of Sample

The samples were then freeze-dried. During freeze-drying, measurements were taken of specimen temperatures, specimen weight change and time.

After completion of freeze-drying, rehydration experiments were conducted on the cube samples. It was desired to determine the effect of varying several parameters on rehydration.

One of the variables was the extent of freeze-drying. Some samples were freeze-dried only until there was no further weight-loss. Other samples were left in the

freeze-drying chamber for a period of time after the indication that weight loss had stopped.

Another variable was the time elapsed between the completion of freeze-drying and the rehydration process. Some samples were rehydrated immediately following the completion of freeze-drying. Other samples were exposed to the atmosphere for a period of time between freeze-drying and rehydration.

Another variable was the temperature at which rehydration occurred. Rehydration temperatures ranged from 40°F to 212°F.

Another variable was rehydration time. The specimens were rehydrated for various periods of time varying from one second to three minutes. Following each rehydration the specimen was weighed.

C. EXPERIMENTAL RESULTS

1. Discrete Frozen Front

An experiment was conducted in an attempt to verify or refute the analytical conclusion of a discrete sublimation front.

A turkey slice described in Section V.B. was imbedded with four thermocouples placed at even intervals in the approximately one centimeter thick slice [Fig. 14]. The results are shown in Figure 15 and Figure 16 which are observed to be similar to Figure 1 and Figure 2.

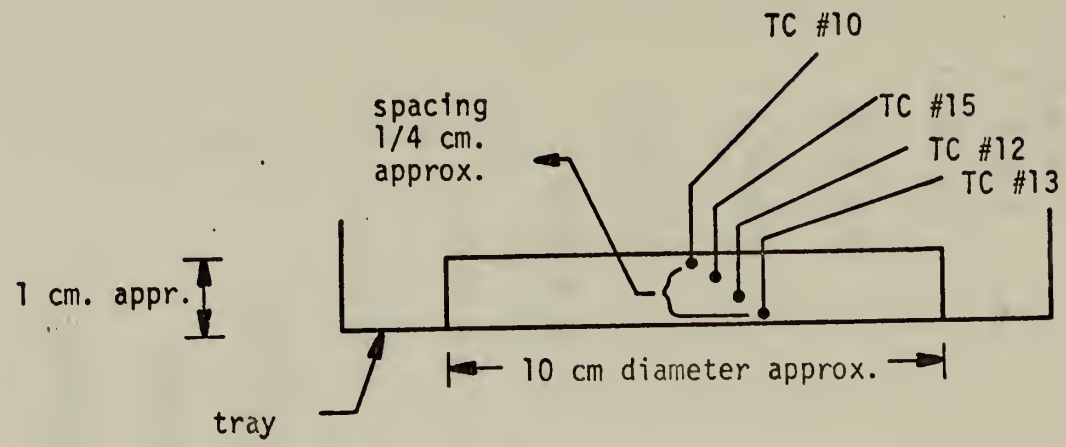

Figure 14. Thermocouple location in one-dimensional freeze-drying and rehydration, specimen slice

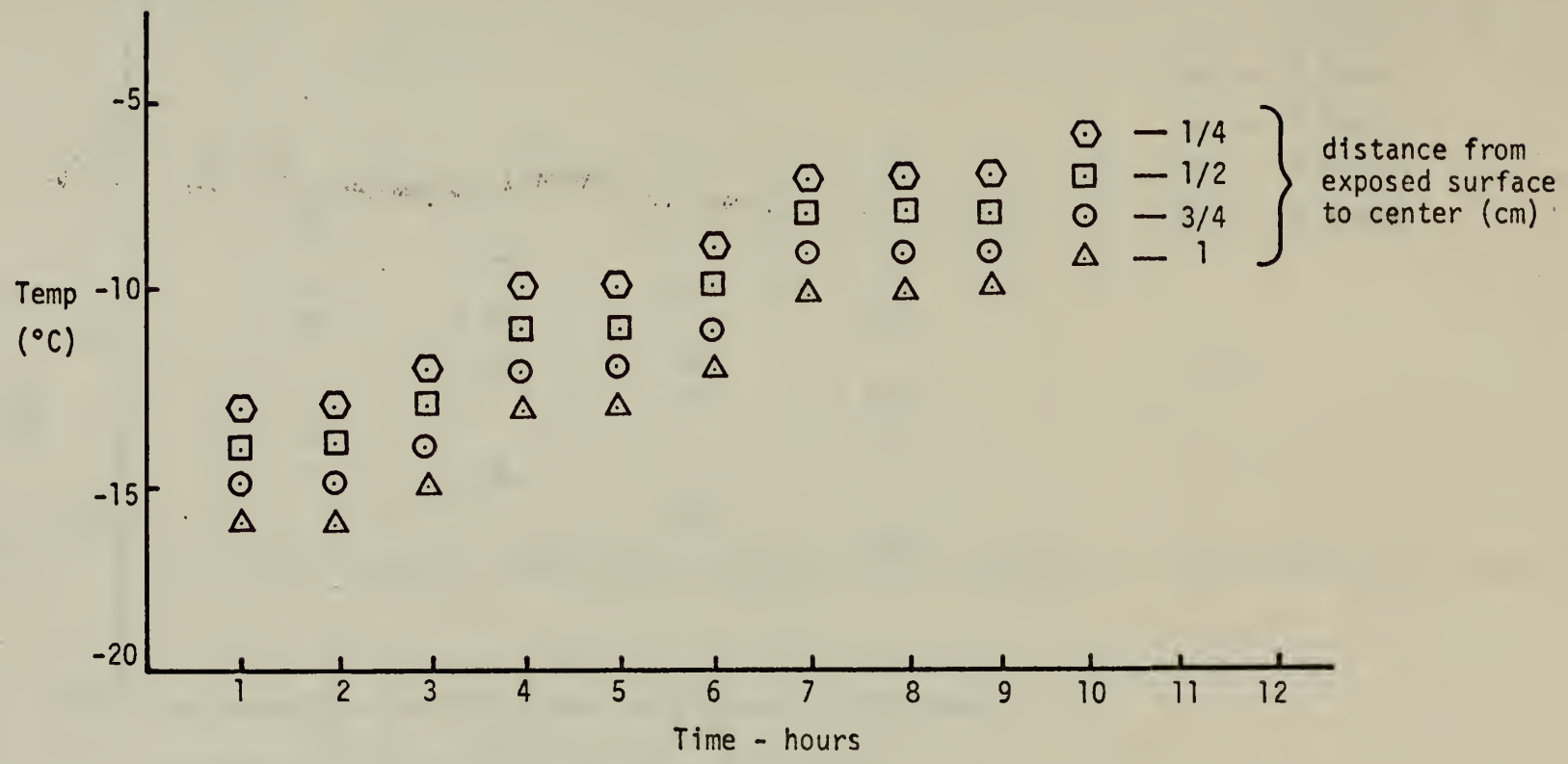

Figure 15. Temperature versus time at different thermocouple locations during the freeze-drying of turkey.

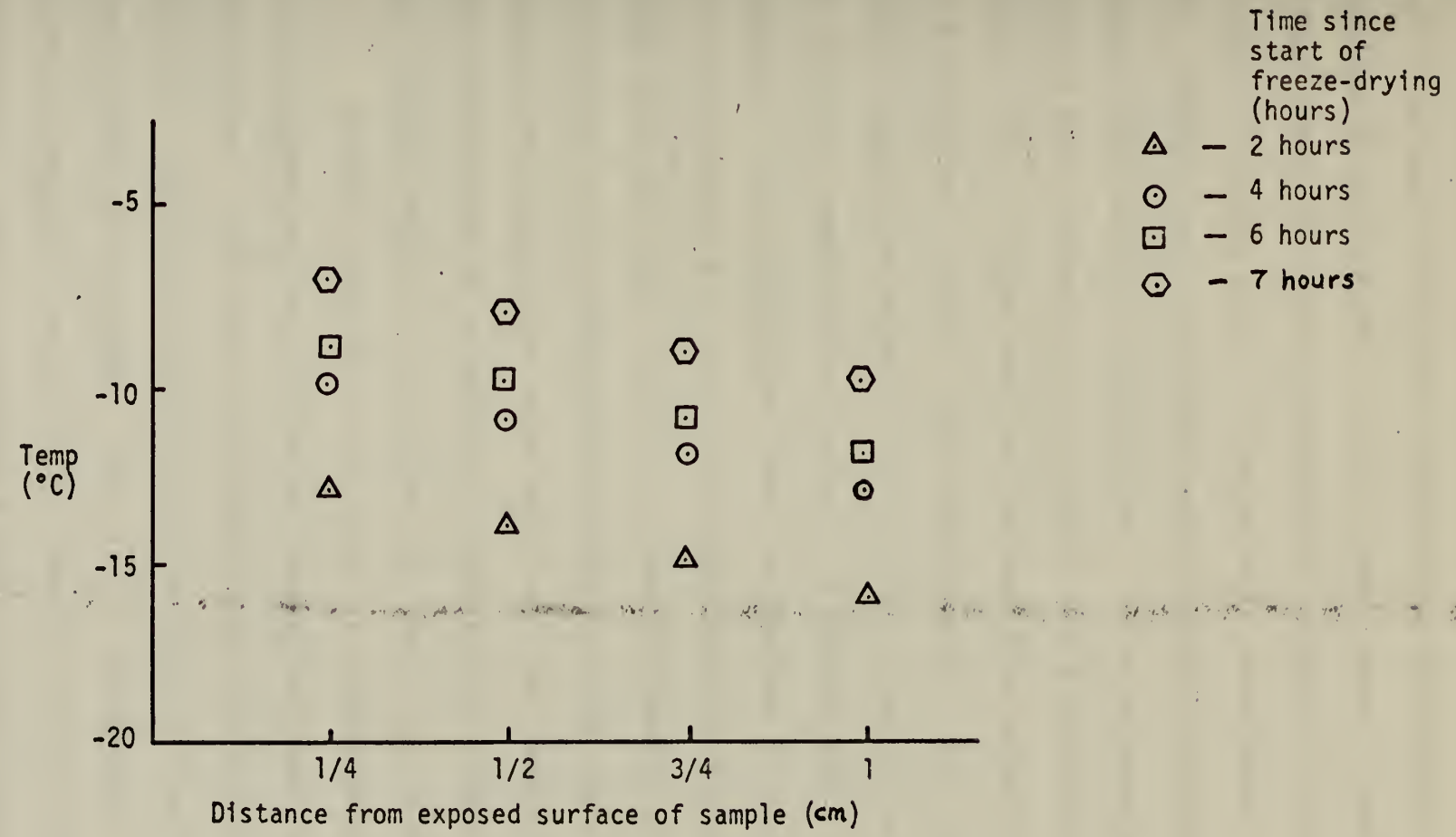

Figure 16. Temperatures versus position at different times during the freeze-drying of turkey

Figures 15 and 16 are not as dramatic as Figures 1 and 2 because of several significant differences in the experimental procedures. In the experiments conducted by Hatcher [Ref. 19], the thermocouple separation distances are several times greater than in this experiment. Furthermore, Hatcher used a variable heat source to maintain a constant high surface temperature. In this experiment, the constant heat source of the chamber walls resulted in a slowly rising surface temperature and thus slowly rising ice temperature and dry layer temperature. This slowly rising temperature makes it difficult to determine whether the observed temperature increase is indeed due to the passing of the sublimation front or whether it is simply the sample heating up due to an imbalance in the rates of energy gain and loss. Adding to the difficulty of discerning the passing of the sublimation front are the facts that the temperature changes are very small and the temperature measuring system is relatively insensitive to small temperature changes which in this case are very significant.

Another problem in the area of temperatures is the disparity between the indicated temperature and the actual temperature. Note that the temperature profile is never constant. Instead a gradient exists with the warmer temperatures toward the surface. This is to be expected, but only after the sublimation front has passed. It is felt that the thermocouple lead is conducting heat to the thermocouple bead causing it to indicate a higher temperature than

actually exists. Furthermore, any opening alongside the thermocouple lead would permit the entrance of vapor and warm air or would be a surface through which freeze-drying could occur resulting in a higher temperature at the thermocouple bead.

2. The Freeze-Drying Model – The Uniformly Retreating Ice Front (URIF)

An experiment was conducted in order to verify or refute the analytical freeze-drying model.

A turkey slice described in Section V.B. was placed on the weight-change indication device and freeze-dried.

It is anticipated from Equation (13) that a plot of (1-x) versus $\frac{T_e - T_f}{-(\frac{dx}{d\theta})}$ would be linear. Since T_e and T_f are essentially constant during the removal of the first 85% of the water, Equation (13) may be integrated with a constant $(T_e - T_f)$ resulting in the following form:

$$(1-x) = \frac{8kV_w}{\Delta H_s L^2} (T_e - T_f) \left\{ \frac{\theta}{1-x} \right\} - \frac{4}{L} \frac{k}{h} \qquad (30)$$

Thus a plot of (1-x) versus $\frac{\theta}{1-x}$ should result in a straight line for the removal of the first 85% of the water. Such a linear plot would suggest adherence of the experimental results to the analytical model.

Figure 17 is a plot of 1-x versus $\frac{\theta}{1-x}$ for the turkey slice previously mentioned. The curve is essentially linear

for the first 85% of weight loss verifying the validity of the analytical model employing the Uniformly Retreating Ice Front (URIF).

3. Rehydration

For the experimental evaluation of the rehydration model a Rehydration Number and Rehydration Ratio are defined.

Let

M_o = mass before freeze-drying

and

M_d = mass after freeze-drying

Then

$M_{w_x} = M_o - M_d$ = mass of water removed during freeze-drying

Assume that

M_{w_x} = maximum amount of water to be absorbed in rehydration

Let

M_w = mass of water absorbed at any time after rehydration has begun

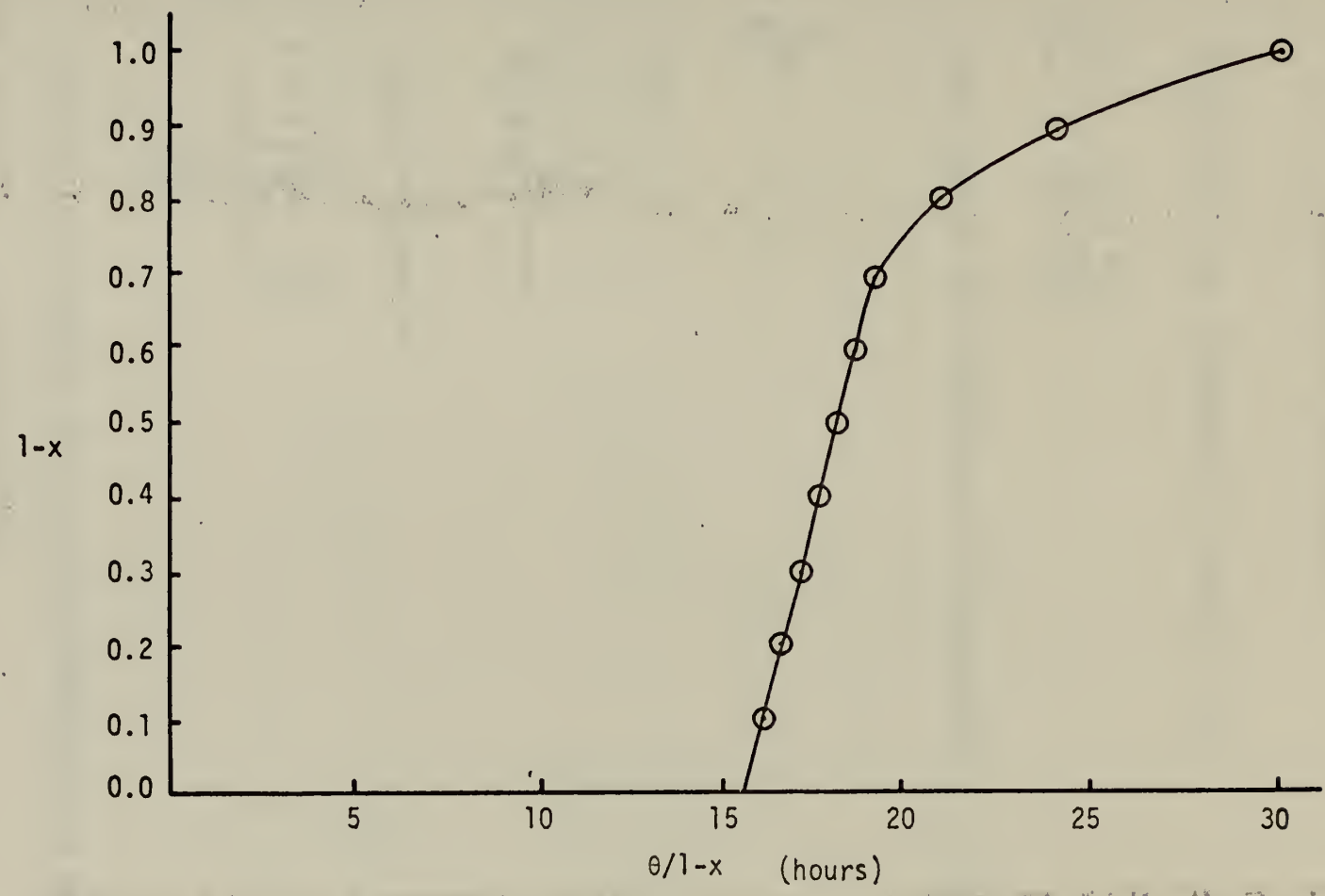

Figure 17. (1-x) versus θ/(1-x) during the freeze-drying of turkey

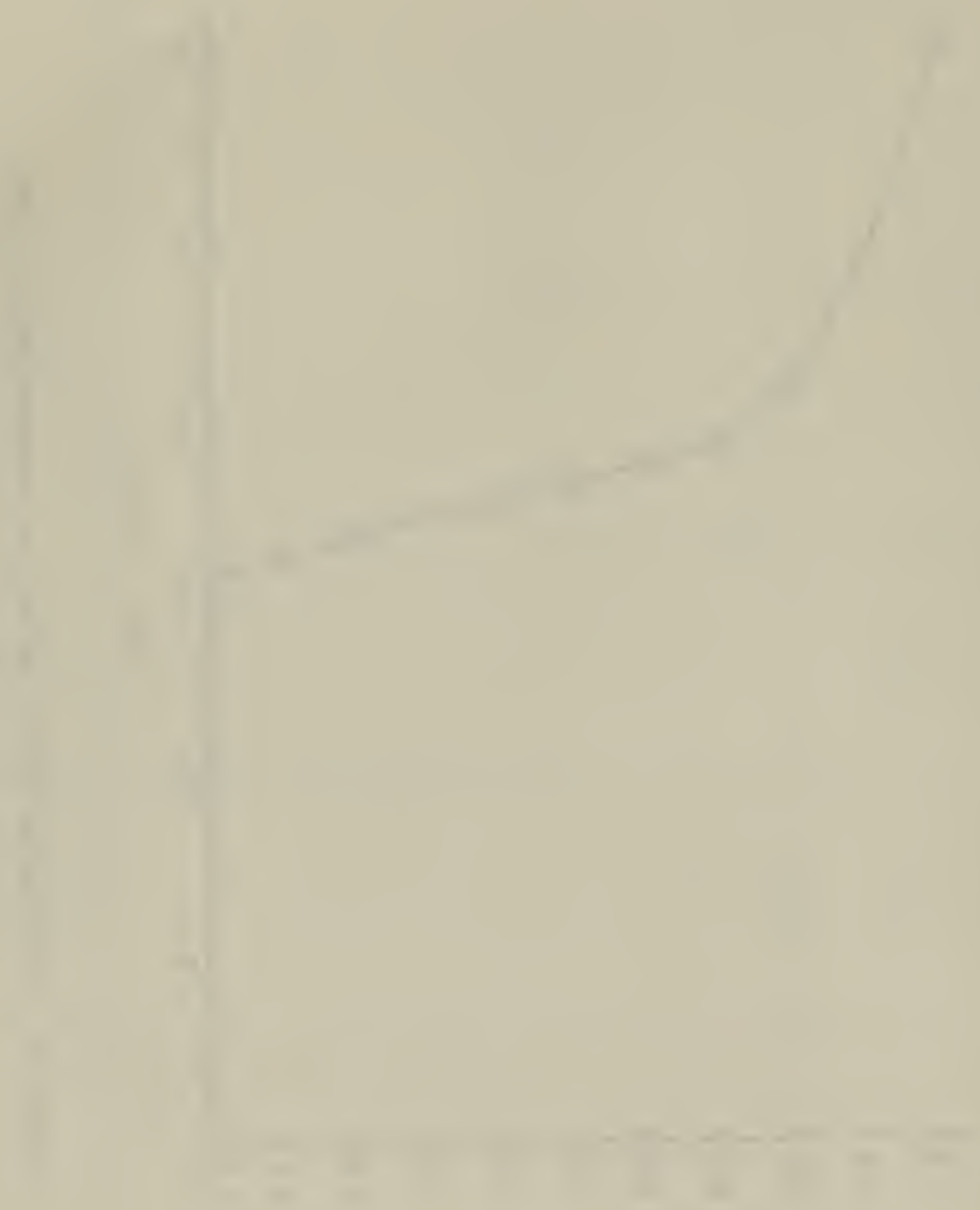

And

$M = M_d + M_w$ = mass of specimen at any time after rehydration has begun

Now define the Rehydration Number, R_H,

$$R_H = \frac{M}{M_o} = \frac{M_d + M_w}{M_d + M_{w_x}} \tag{30}$$

Next define the fraction of rehydration, r, such that

$$r = \frac{M_w}{M_{w_x}} \tag{31}$$

Thus

$$R_H = \frac{M_d + r M_{w_x}}{M_d + M_{wx}} \tag{32}$$

which reduces to

$$R_H = \frac{1 + r\left(\frac{M_o}{M_d} - 1\right)}{\frac{M_o}{M_d}} \tag{33}$$

Define the minimum value of the Rehydration Number, that is, when $M = M_d$, as R_{HD}, thus

$$R_{HD} = \frac{M_d}{M_o} \tag{34}$$

Now

$$R_H = \frac{1 + r\left(\frac{1}{R_{HD}} - 1\right)}{1 + \frac{1}{R_{HD}} - 1} \qquad (35)$$

which reduces to

$$R_H = R_{HD} + r(1 - R_{HD}) \qquad (36)$$

where $(1 - R_{HD})$ is the fraction of water in the original mass before freeze-drying and $r(1 - R_{HD})$ is the fraction of water in the mass at any time during rehydration.

Thus, Equation (36) may be written verbally as

FRACTION OF THE ORIGINAL (BEFORE FREEZE-DRYING) MASS AT ANY TIME	=	FRACTION OF THE ORIGINAL MASS THAT IS DRY	+	FRACTION (r) OF THE FRACTION OF THIS ORIGINAL MASS THAT WAS WATER
(WATER + DRY SUBSTANCE - FUNCTION OF TIME)	=	(DRY SUBSTANCE - CONSTANT)	+	(WATER - FUNCTION OF TIME)

Referring to Figure 8 and assuming that the capillary diameter remains constant, Equation (31) becomes

$$r = \frac{M_w}{M_{w_x}} = \frac{h}{L} \qquad (37)$$

Dividing through both sides of Equation (29) by L_1^2 yields

$$r^2 = \frac{h_1^2}{L_1^2} = \frac{d\gamma g_c t}{4\mu L_1^2} \tag{38}$$

Note that for a given geometry, the fraction of rehydration, r, is directly proportional to the square root of the ratio of $(\frac{\gamma}{\mu})$. This term, which incorporates all of the fluid properties influence on r, is a function of temperature, and is tabulated at the end of Appendix B. From this data, the theoretical model predicts a significant increase in rehydration with increasing temperature.

Now define the Rehydration Ratio, $\frac{R_H}{R_{HD}}$, as

$$\frac{R_H}{R_{HD}} = \frac{\frac{M}{M_o}}{\frac{M_d}{M_o}} = \frac{M}{M_o \frac{M_d}{M_o}} = \frac{M}{M_d} \tag{39}$$

Tables 1-4 and 6-9 contain the experimental and reduced data resulting from four different batch-runs.

In each case the samples were prepared and processed as outlined in Section B.1.

After normal processing Batch #1 (Tray #7) was freeze-dried for an additional seven days beyond indication that weight removal had stopped. Batch #1 was then removed from the freeze-drier and rehydrated.

After normal processing Batch #2 (Tray #8) was removed from the freeze-drying process, wrapped in two plastic bags and left out in the atmosphere. After one week of exposure to the atmosphere Batch #2 was rehydrated.

After normal processing Batch #3 (Yellow Tray) was removed from the freeze-dryer and rehydrated immediately.

Batches #1, #2, and #3 were rehydrated at temperatures of 40°F, 80°F, 100°F, 120°F, 160°F, and 212°F. The specific temperatures used depended upon batch size and temperature ranges examined. Because of the large piece-to-piece variation in sample specimens it was felt that a minimum of three specimen pieces was essential for each set of conditions examined.

After reducing the data for Batches #1, #2, and #3, and determining that the most effective rehydration temperatures were the higher temperatures, Batch #4 (Green Tray) was processed and freeze-dried normally and then rehydrated at the higher temperatures; 160°F, 180°F, 212°F (simmer) and 212°F (vigorous boil).

In all cases rehydration was performed by immersing the specimen in water for one, two, three, four, five, ten, fifteen, thirty, sixty, one hundred twenty, and one hundred eighty seconds. The specimen was weighed after each rehydration immersion.

The significant difference of rehydration ratios between batches emphasizes the necessity for proper processing in order to attain maximum rehydration.

Batch #3 which was freeze-dried until there was no further weight loss and then immediately rehydrated shows the highest rehydration ratio. In comparison, Batch #1, which was freeze-dried beyond the time of no further weight loss and rehydrated immediately shows a significantly reduced rehydration ratio. Thus "over-drying" must be avoided if maximum rehydration ratio is to be attained.

Batch #2 was freeze-dried until there was no further weight-loss, but left exposed to the atmosphere prior to rehydration. The resulting reduction in rehydration ratio is significant. Thus "case hardening" must be avoided if maximum rehydration is to be attained.

Even Batch #4 which was freeze-dried until there was no further weight loss and almost immediately rehydrated shows a reduced rehydration ratio. Despite extensive packaging, indications are that case hardening occurred prior to rehydration.

A comparison of rehydration ratios within batches points to some significant conclusions. In the cases of improperly processed samples, results from Batches #1 and #2 indicate that the higher rehydration temperatures result in the higher rehydration ratios. Thus the "over-drying" and "case-hardening" problems are best relieved by high temperature rehydration or "re-cooking".

A comparison of rehydration ratios within Batch #3 reveals no conclusive trends. If a conclusion were drawn it might be that the middle temperatures afforded the highest rehydration ratio.

Batch #4 was rehydrated over a range of high temperatures including boiling; both simmering and vigorous boiling. Results do not indicate conclusively an obvious optimum rehydration temperature. It does seem indicative that a hard boil is preferential to a simmer. The somewhat obvious conclusion from Batch #4 that 180°F is the most optimum temperature for maximum rehydration ratio is not reinforced with the inconclusive results from Batch #3.

The rehydration model predicted an increased rehydration ratio with increased temperature. This prediction is very strongly verified by the experimental data. In the batches of "case-hardened" and "over-cooked" specimens the model prediction is the only trend noted.

For the batches of specimens that were freeze-dried only until weight loss stopped and then immediately rehydrated, the trend is not as significant. There is an increase in rehydration ratio with increasing temperature up to the range of 120°F - 160°F. At higher temperatures rehydration ratio decreases. This agrees with findings of other researchers in this field who found a "protein denaturation" effect above 180°F.

The analytical rehydration model predicts that rehydration rate would follow a second order curve for one dimensional rehydration. Furthermore, the analysis predicts that rehydration occurs in about one second in a sample one centimeter long in the capillary direction and that

rehydration occurs in between four and five seconds for a sample approximately 2.2 cm long in the capillary direction.

Tables 5 and 10-12 contain the experimental and reduced data resulting from four one-dimensional samples.

Four turkey meat slices approximately 2.2 centimeters thick by ten centimeters in diameter were freeze-dried until there was no further weight loss and then immediately rehydrated in 120°F water.

Samples #1 and #3 were rehydrated in a horizontal position (capillaries vertical) and Samples #2 and #4 were rehydrated in a vertical position (capillaries horizontal).

As the model predicted rehydration occurs very rapidly. Specifically, the model predicted that for a sample of 2.2 centimeters thickness in the capillary direction, rehydration should occur in approximately four to five seconds.

Figure 18 is a plot of fraction of rehydration, r, versus time. Figure 18a is a plot of rehydration number, $R_H = \frac{M}{M_o}$, versus time. Figure 18b is a plot of rehydration ratio versus time.

The experimental results suggest that of the total amount of water that is eventually rehydrated, a fraction (about 80%) is rehydrated in the first few seconds. An obvious break occurs in the experimental curves in Figure 18 at about r = 0.5, which is approximately 80% of the r at three minutes. Prior to this point, at approximately t = 3 seconds, it appears that rehydration follows the model

of capillary rehydration. After 3 seconds the rehydration rate slows significantly, indicating that the large capillaries are filled. The subsequent rehydration would seem to be the much slower soaking of the previously dry myofibrils. The decreased rehydration rate would seem to be due to the smaller effective diameter capillaries.

Thus for purposes of comparing the experimental results with the rehydration model, the experimental results should be normalized. This will result in experimental curves based on only the water which is rehydrated due to primary capillary action, which is the basis for the model.

Figure 19 is the comparison of the theoretical curve and the normalized experimental curves. Since the break is observed to occur at a $r \approx 0.5$, the normalized curves are obtained by dividing r by 0.5. It is observed that the experimental curves strongly verify the rehydration model. In addition they specifically suggest an effective capillary diameter of 0.0010 cm.

From the figures it is observed that the difference between rehydration ratios of the specimens rehydrated horizontally and those rehydrated vertically is insignificant. The percentage difference in rehydration ratios is less than four percent. Thus the experimental results verify the prediction of the rehydration model that the effect of gravity on rehydration was insignificant.

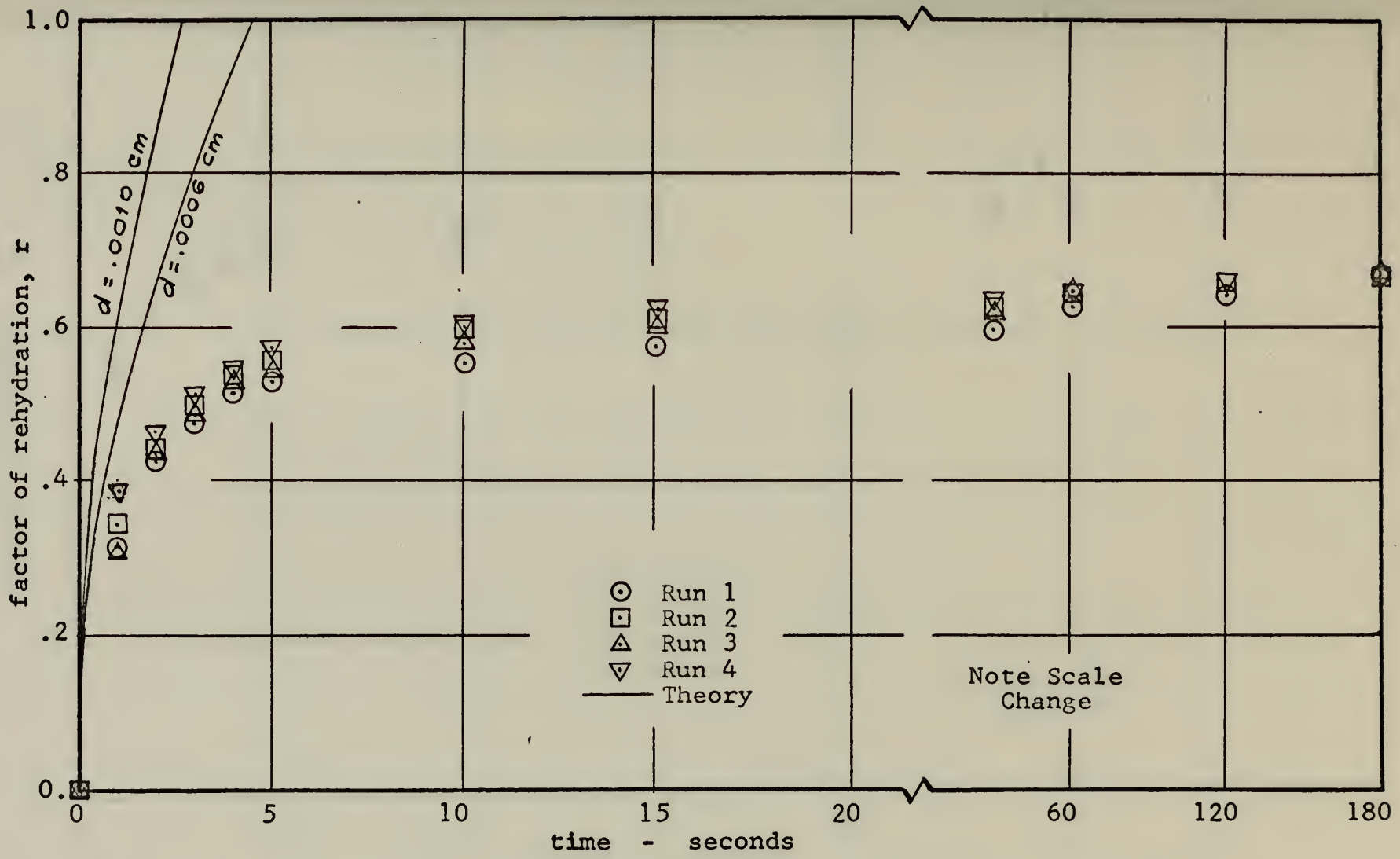

Figure 18. Fraction of rehydration, r, as a function of time. (Batch #5)

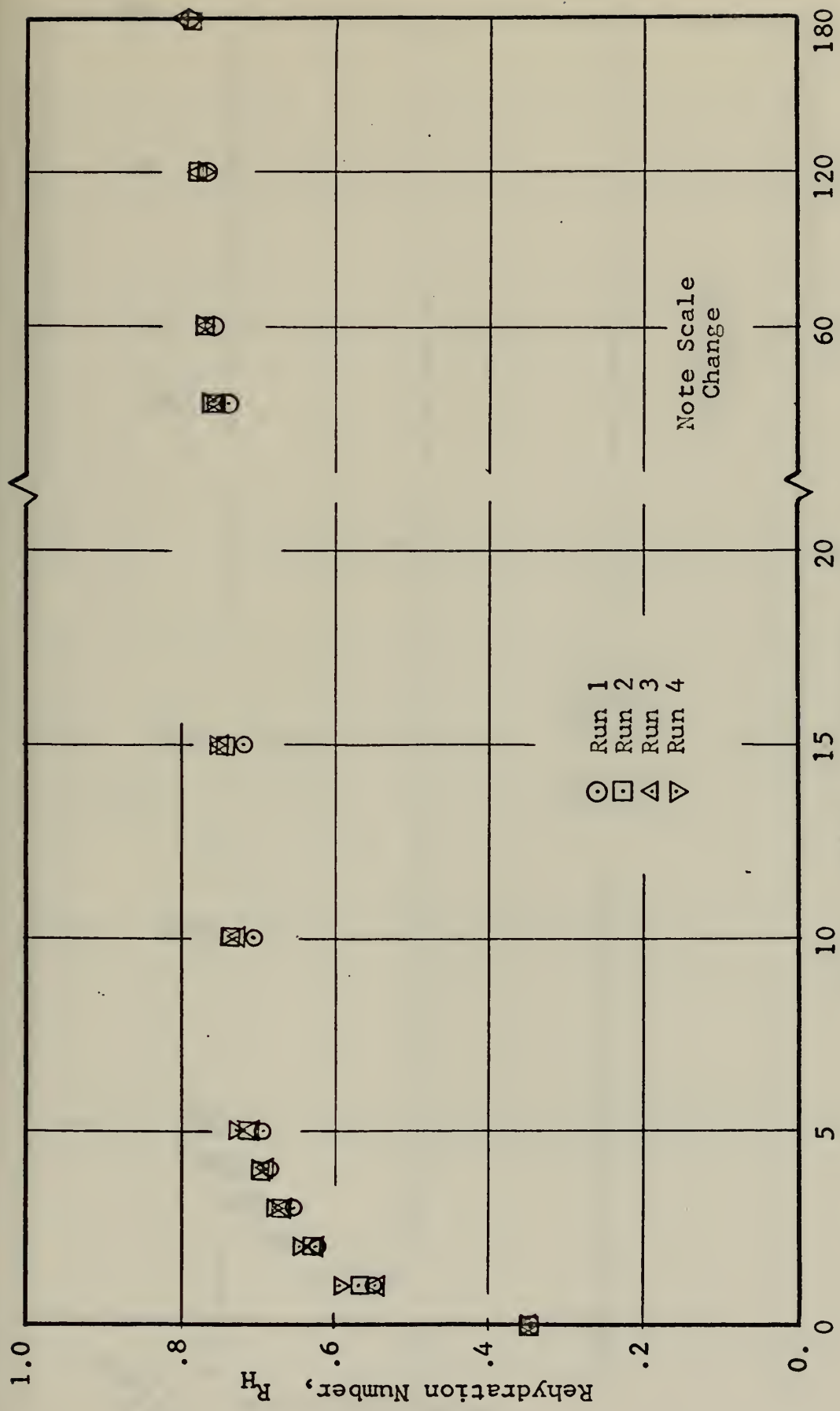

Figure 18a. Rehydration number, M/M_o, as a function of time (Batch #5)

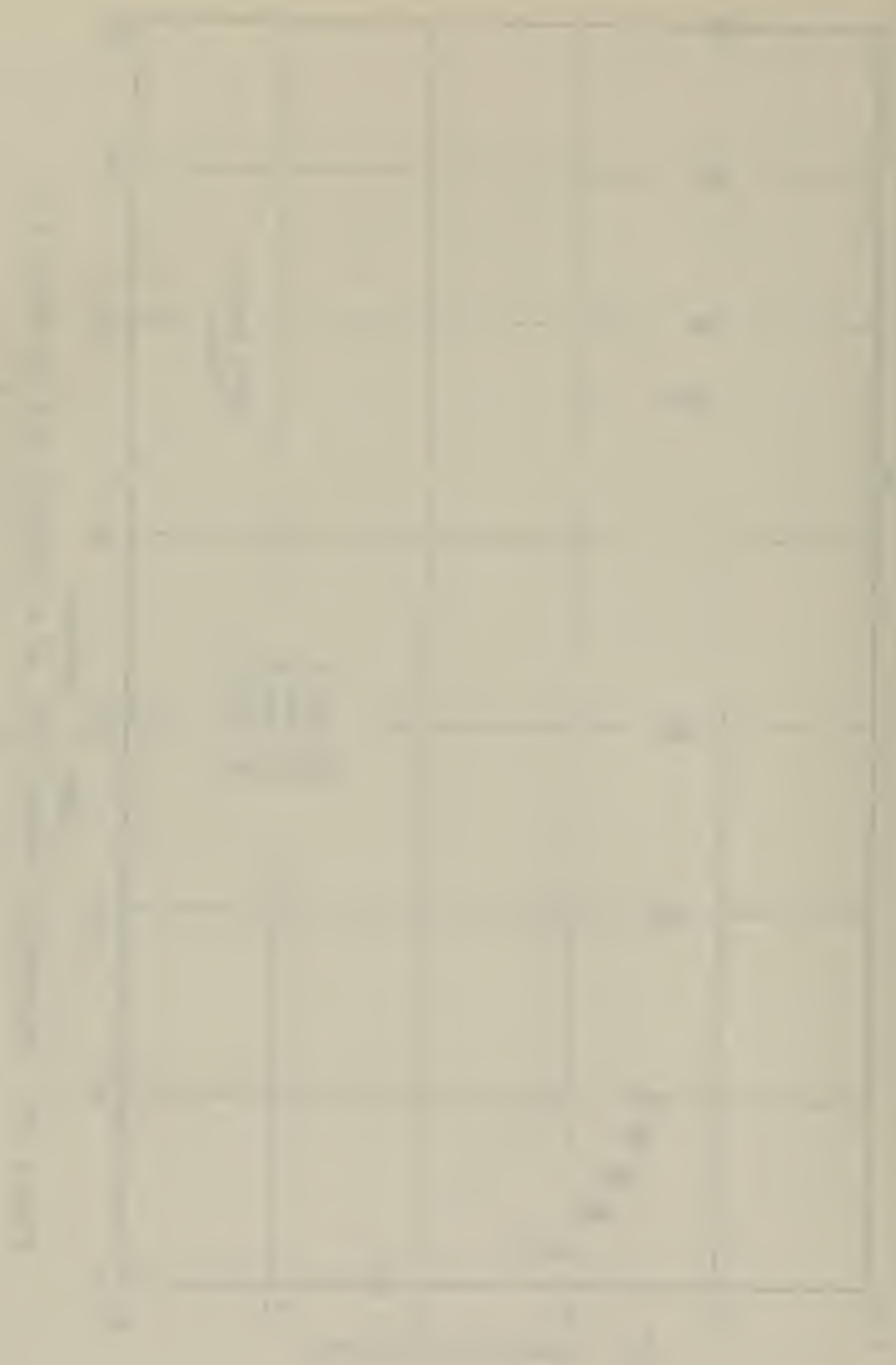

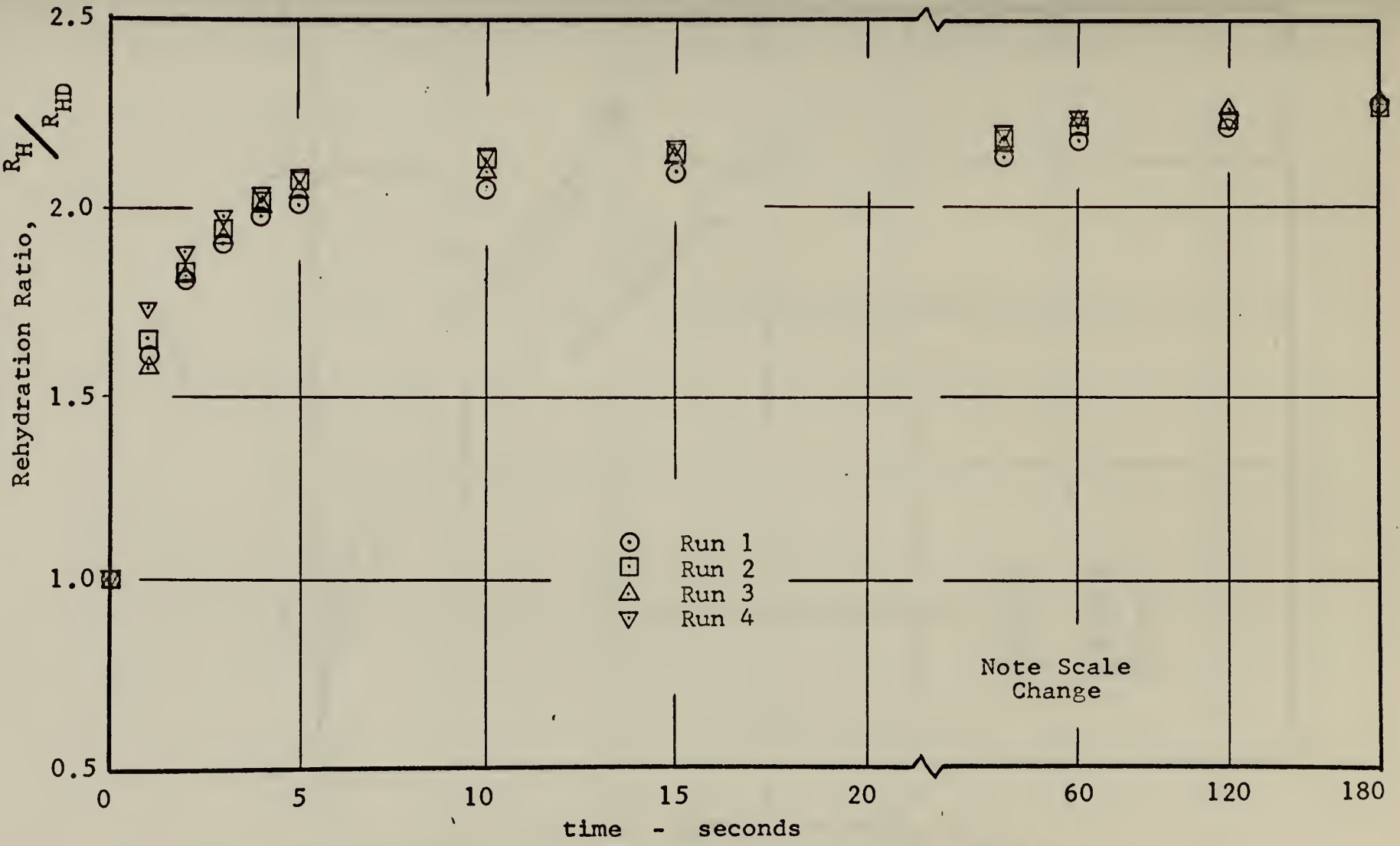

Figure 18b. Rehydration rate, R_H/R_{HD}, as a function of time (Batch #5)

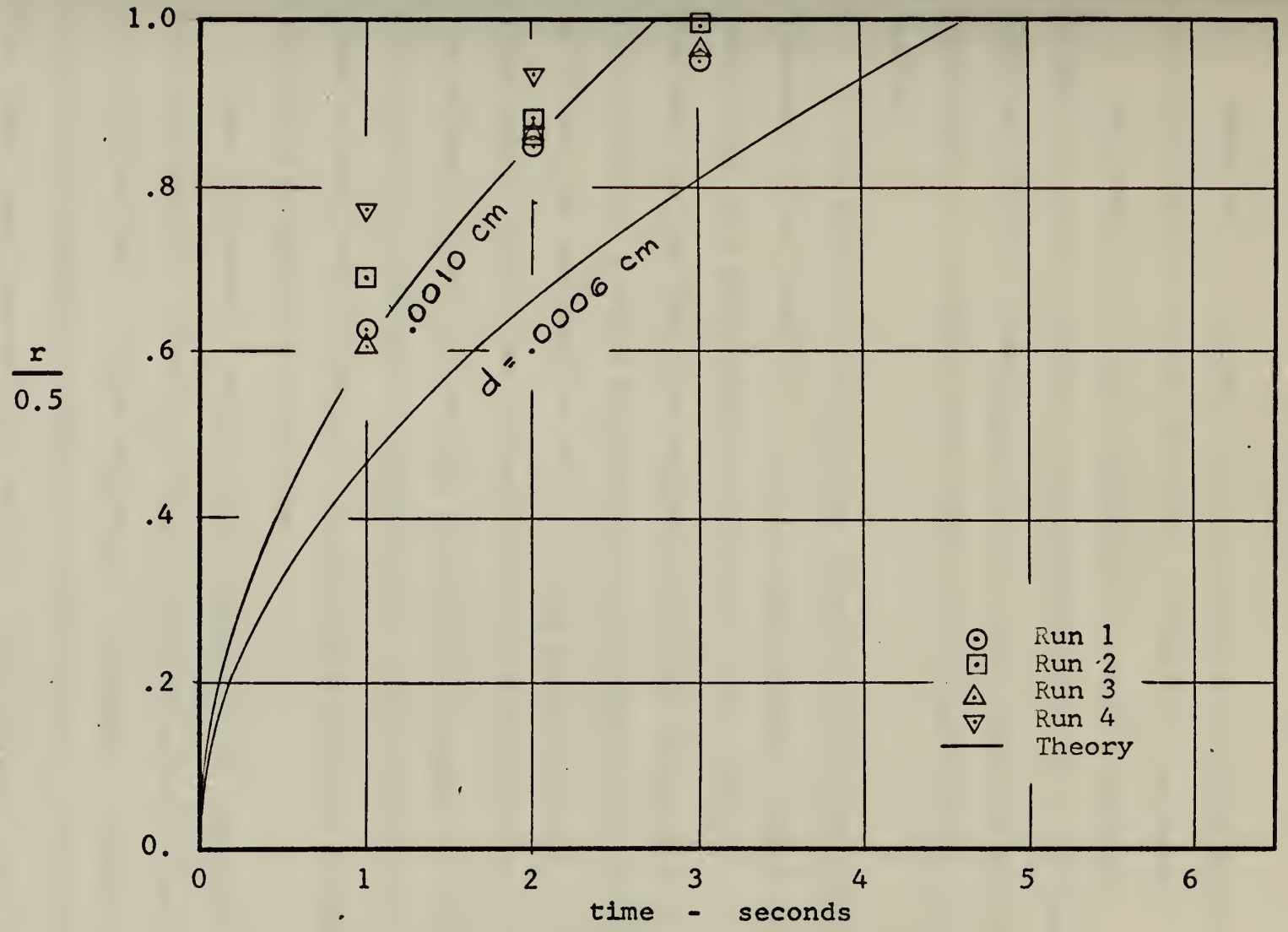

Figure 19. r/0.5 as a function of time (Batch #5)

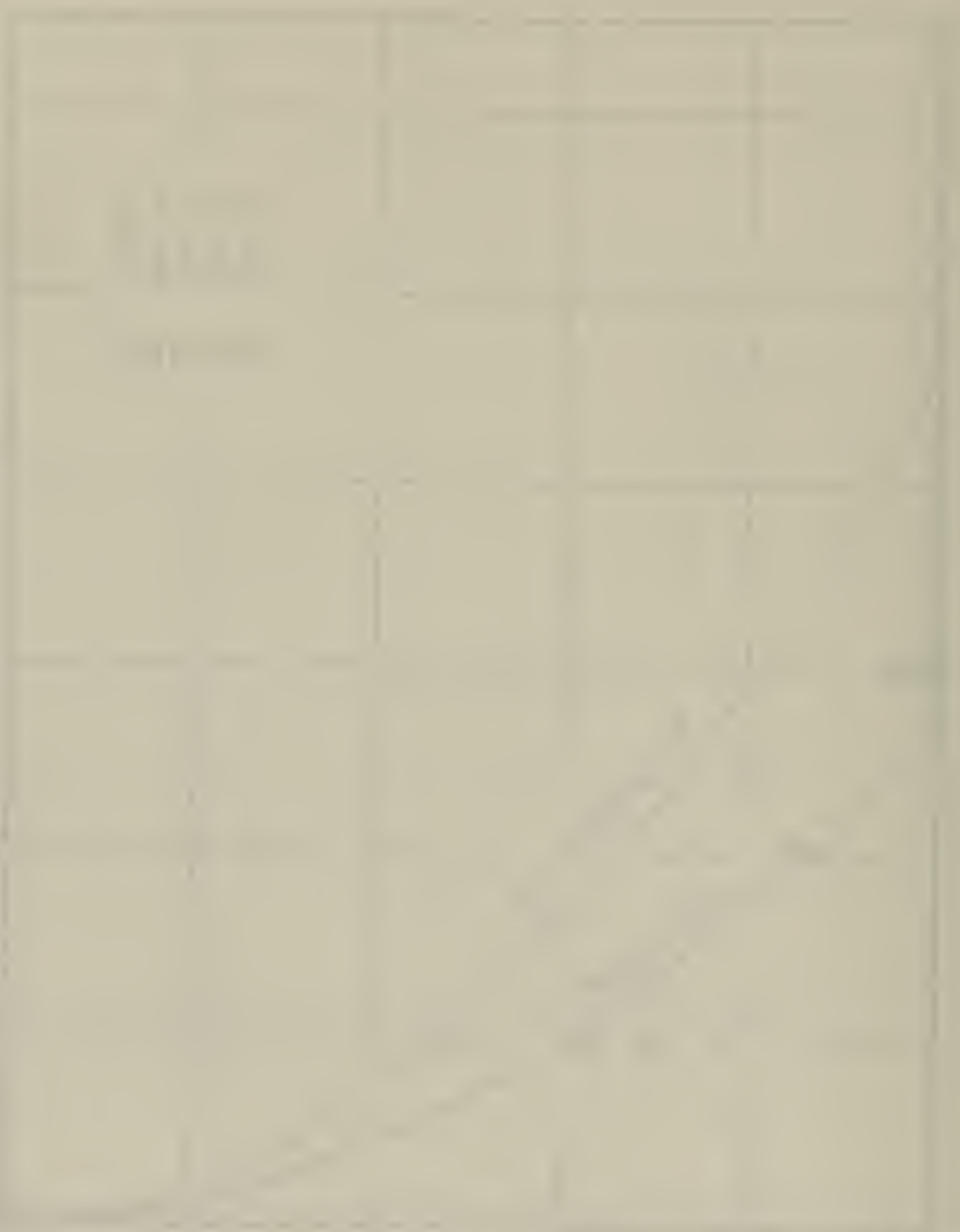

VI. CONCLUSION

Based on the above studies of both an analytical and an experimental nature, several conclusions are made.

Both analytical and experimental results strongly suggest that the nature of the frozen front is a discrete and not a diffuse sublimation front, and that the Uniformly Retreating Ice Front (URIF) Model for freeze-drying is valid.

In the areas of rehydration there is less definition because of the dearth of work in these areas. Based on the analytical and experimental results of this author, indications are that the rehydration model developed in this paper is a valid approximation. Experimental results verified the rehydration model in the prediction of rehydration rates, the assumption of the insignificance of the effect of gravity and the anticipated change of rehydration rate with change in temperature. The experimental results compared favorably with the model with an effective capillary diameter of 0.0010 cm.

From the general rehydration studies it is concluded that rehydration ratios increase with increasing temperature for "over-dried" or "case-hardened" specimens. Temperature effects on rehydration ratios are inconclusive for specimens that have been freeze-dried without "over-drying" and immediately rehydrated without "case-hardening."

Of significance, it should be noted that the newly developed rehydration model accurately predicts rehydration rates for the first 80-85% of rehydration. Recall that the freeze-drying model also accurately predicted freeze-drying rates for the first 80-85% of freeze-drying.

It is apparent that during the last 15-20% of both freeze-drying and rehydration secondary effects become significant causing the observed deviations from the model predictions.

Rehydration Rates by Weight — Batch #1 - Tray #7

	Before Freeze Drying	Before Rehyd.	After Rehydrating 1 sec	2 sec	3 sec	4 sec	5 sec	10 sec	15 sec	30 sec	1 min	2 min	3 min	Temp
1)	7.1	2.6	3.4	3.7	3.8	3.9	4.0	4.2	4.2	4.2	4.2	4.2	4.2	40
2)	5.45	1.9	2.6	3.0	3.1	3.2	3.2	3.2	3.2	3.2	3.2	3.2	3.2	40
3)	6.4	2.4	3.3	3.7	3.9	3.9	3.9	3.9	3.9	3.9	3.9	3.9	3.9	40
4)	2.4	3.3	3.5	3.6	3.6	3.6	3.6	3.6	3.6	3.6	3.7	3.7	3.7	80
5)	5.9	2.1	3.2	3.5	3.5	3.5	3.5	3.6	3.7	3.7	3.7	3.7	3.7	80
6)	4.8	1.6	2.6	3.0	3.1	3.1	3.1	3.1	3.1	3.1	3.1	3.1	3.1	80
7)	4.7	1.8	2.5	2.5	2.5	2.5	2.5	2.5	2.6	2.7	2.7	2.7	2.7	120
8)	7.2	2.6	4.1	4.3	4.4	4.5	4.6	4.6	4.6	4.6	4.6	4.6	4.6	120
9)	6.05	2.3	3.5	3.6	3.6	3.7	3.8	3.9	4.0	4.0	4.0	4.2	4.2	160
10)	6.4	2.3	3.7	4.0	4.1	4.2	4.3	4.3	4.4	4.6	4.6	4.7	4.8	160
11)	5.05	1.9	2.7	2.9	3.0	3.1	3.2	3.2	3.2	3.3	3.4	3.4	3.4	160
12)	5.7	2.1	2.9	3.1	3.2	3.3	3.4	3.5	3.6	3.6	3.9	4.4	4.8	212
13)	6.2	2.2	3.4	3.8	4.0	4.3	4.3	4.4	4.5	4.6	4.6	4.6	5.0	212
14)	7.6	2.8	3.4	3.8	4.0	4.0	4.1	4.1	4.3	4.4	4.5	4.7	4.8	212

No Boil

TABLE 1. Rehydration Rate versus time, Batch #1

Rehydration Rates by Weight — Batch #2

	Before Freeze Drying	Before Rehyd.	After Rehydrating 1 sec	2 sec	3 sec	4 sec	5 sec	10 sec	15 sec	30 sec	1 min	2 min	3 min	Temp
1)	6.3	2.4	2.8	3.1	3.3	3.3	3.3	3.3	3.3	3.3	3.3	3.3	3.3	40
2)	6.5	2.6	2.7	2.8	3.0	3.1	3.1	3.1	3.1	3.1	3.1	3.1	3.1	40
3)	7.6	3.2	3.3	3.5	3.7	3.8	3.9	3.95	3.95	4.0	4.1	4.15	4.15	40
4)	6.9	2.8	3.5	4.0	4.1	4.1	4.2	4.3	4.4	4.5	4.5	4.6	4.7	80
5)	7.8	3.0	3.4	3.8	4.0	4.2	4.2	4.3	4.4	4.4	4.4	4.5	4.6	80
6)	7.4	2.9	3.2	3.5	3.7	3.7	3.8	3.9	3.9	3.9	4.0	4.2	4.2	80
7)	7.3	2.9	3.4	3.8	4.0	4.1	4.15	4.3	4.4	4.4	4.4	4.5	4.6	120
8)	5.6	2.1	2.3	2.4	2.5	2.6	2.7	2.7	2.7	2.7	2.8	2.9	3.0	120
9)	6.2	2.4	2.9	3.0	3.1	3.2	3.25	3.3	3.4	3.4	3.45	3.55	3.7	160
10)	5.1	1.7	2.0	2.3	2.4	2.5	2.6	2.7	2.7	2.75	2.75	2.75	2.75	160
11)	5.1	2.2	2.7	2.9	3.1	3.3	3.4	3.4	3.4	3.4	3.5	3.7	3.9	160
12)	3.9	1.6	2.2	2.4	2.5	2.6	2.6	2.6	2.6	2.6	2.65	2.8	3.0	212
13)	5.1	2.1	2.4	2.6	2.7	2.75	2.8	2.8	2.8	2.9	2.9	2.95	3.05	212
14)	4.6	1.8	2.1	2.5	2.7	2.8	2.9	3.0	3.0	3.05	3.1	3.2	3.4	212

TABLE 2. Rehydration Weight versus time; Batch 2

Rehydration Rates by Weight (GMS) Batch #3

	Before Freeze Drying	Before Rehyd.	After Rehydrating 1 sec	2 sec	3 sec	4 sec	5 sec	10 sec	15 sec	30 sec	1 min	2 min	3 min	Temp
1)	6.0	2.0	3.1	3.5	3.6	3.7	3.8	4.0	4.1	4.2	4.3	4.4	4.5	40
2)	7.2	2.5	4.1	4.7	5.0	5.3	5.5	5.7	5.8	6.2	6.2	6.2	6.2	40
3)	8.4	2.9	4.3	5.0	5.4	5.5	5.7	5.9	6.1	6.2	6.2	6.2	6.2	40
4)	6.5	2.3	4.1	4.8	5.1	5.3	5.7	5.7	5.7	5.7	6.0	6.0	6.0	100
5)	6.2	2.1	3.9	4.4	4.9	5.0	5.0	5.3	5.3	5.4	5.5	5.6	5.6	100
6)	5.8	2.0	3.8	4.2	4.5	4.6	4.6	4.6	4.6	4.7	4.8	4.9	4.9	100
7)	5.9	1.6	2.8	3.3	3.4	3.6	3.6	3.6	3.6	3.9	3.9	3.9	3.9	160
8)	5.6	2.0	3.5	3.9	4.2	4.4	4.5	4.5	4.5	4.8	4.8	4.9	5.0	160
9)	8.1	2.9	4.6	5.2	5.5	5.7	5.8	6.0	6.2	6.5	6.7	7.0	7.0	160
10)	7.4	2.6	4.3	4.9	5.2	5.4	5.6	5.9	6.0	6.0	6.1	6.2	6.2	212
11)	6.9	2.4	4.0	4.4	4.7	4.8	4.8	4.9	4.9	5.0	5.1	5.1	5.1	212
12)	4.9	1.6	2.8	3.4	3.5	3.7	3.8	3.8	3.9	4.1	4.1	4.1	4.1	212

TABLE 3. Rehydration Rate versus time; Batch #3

Rehydration Rates by Weight (GMS) Batch #4 - Green Tray

	Before Freeze Drying	Before Rehyd.	After Rehydrating 1 sec	2 sec	3 sec	4 sec	5 sec	10 sec	15 sec	30 sec	1 min	2 min	3 min	Temp
1)	5.2	1.8	2.9	3.0	3.3	3.3	3.4	3.5	3.6	3.6	3.7	3.9	4.1	212
2)	5.1	1.8	2.8	3.1	3.3	3.3	3.5	3.6	3.7	3.8	4.0	4.0	4.0	212
3)	6.0	2.0	3.0	3.3	3.6	3.8	3.9	3.9	4.0	4.1	4.3	4.4	4.6	212
4)	7.1	2.5	4.1	4.4	4.6	4.7	4.9	4.9	5.1	5.1	5.1	5.2	5.3	212
5)	7.1	2.5	3.5	4.1	4.4	4.5	4.8	5.0	5.0	5.0	5.1	5.1	5.1	212
6)	6.6	2.4	3.9	4.4	4.6	4.7	4.8	4.9	4.9	5.1	5.1	5.1	5.1	212
7)	6.0	2.0	3.5	4.0	4.2	4.3	4.5	4.7	4.7	4.7	4.7	4.7	4.7	180
8)	6.2	2.0	3.5	3.9	4.2	4.3	4.4	4.5	4.7	4.8	4.9	5.0	5.0	180
9)	5.7	1.9	3.0	3.3	3.5	3.7	3.7	3.9	4.0	4.0	4.2	4.2	4.3	180
10)	6.5	2.3	4.1	4.4	4.7	4.8	4.8	4.9	4.9	5.0	5.2	5.4	5.6	160
11)	5.9	2.2	3.0	3.3	3.4	3.5	3.5	3.7	3.8	3.8	3.8	3.8	3.8	160
12)	8.5	2.9	4.7	5.2	5.6	5.7	5.9	5.9	6.0	6.2	6.2	6.4	6.6	160

hard boil

simmer

TABLE 4. Rehydration Weight versus time; Batch #4

Rehydration Rates by Weight in grams Batch #5

	Before Rehyd.	1 sec	2 sec	3 sec	4 sec	5 sec	10 sec	15 sec	30 sec	1 min	2 min	3 min	Method; temp=120
1)	18.7	29.9	33.6	35.5	36.8	37.5	38.1	38.9	39.9	40.8	41.3	42.4	horizontal
2)	25.6	42.2	47.0	49.6	51.6	53.0	54.3	54.8	55.9	56.6	57.2	57.8	vertical
3)	30.6	48.2	55.4	58.5	60.9	62.5	64.1	65.1	66.4	67.8	69.1	69.8	horizontal
4)	25.3	43.8	47.5	49.7	51.3	52.8	53.9	54.7	55.5	56.2	56.5	57.2	vertical

TABLE 5. Rehydration Rate versus weight; Batch #5

		1 sec	2 sec	3 sec	4 sec	5 sec	10 sec	15 sec	30 sec	1 min	2 min	3 min	
1)	2.73	1.31	1.42	1.46	1.5	1.6	1.6	1.6	1.6	1.6	1.6	1.6	
2)	2.86	1.37	1.58	1.63	1.68	1.68	1.68	1.68	1.68	1.68	1.68	1.68	1.63
3)	2.66	1.37	1.54	1.62	1.62	1.62	1.62	1.62	1.62	1.62	1.62	1.62	
4)	2.69	1.37	1.46	1.50	1.50	1.50	1.50	1.50	1.50	1.50	1.50	1.50	
5)	2.80	1.52	1.67	1.67	1.67	1.67	1.67	1.67	1.67	1.67	1.67	1.67	1.70
6)	3.00	1.625	1.87	1.94	1.94	1.94	1.94	1.94	1.94	1.94	1.94	1.94	
7)	2.61	1.39	1.39	1.39	1.39	1.39	1.39	1.44	1.5	1.5	1.5	1.5	
8)	2.77	1.58	1.65	1.69	1.73	1.77	1.77	1.77	1.77	1.77	1.77	1.77	1.63
9)	2.63	1.52	1.57	1.57	1.60	1.65	1.70	1.74	1.74	1.74	1.82	1.82	
10)	2.78	1.61	1.74	1.78	1.83	1.87	1.87	1.91	2.0	2.0	2.04	2.09	1.90
11)	2.66	1.42	1.52	1.58	1.63	1.68	1.68	1.68	1.73	1.79	1.79	1.79	
12)	2.71	1.38	1.48	1.52	1.57	1.62	1.66	1.71	1.71	1.86	2.10	2.29	
13)	2.82	1.54	1.73	1.82	1.95,	1.95	2.0	2.05	2.09	2.09	2.09	2.27	2.09
14)	2.71	1.21	1.38	1.43	1.43	1.46	1.46	1.54	1.57	1.61	1.68	1.71	

TABLE 6. Rehydration Ratio, R_H/R_{HD}, as a function of time; Batch #1

		1 sec	2 sec	3 sec	4 sec	5 sec	10 sec	15 sec	30 sec	1 min	2 min	3 min
1)	2.65	1.16	1.29	1.38	1.38	1.38	1.38	1.38	1.38	1.38	1.38	1.38
2)	2.50	1.03	1.08	1.15	1.19	1.19	1.19	1.19	1.19	1.19	1.19	1.19
3)	2.37	1.03	1.09	1.16	1.19	1.22	1.22	1.22	1.25	1.28	1.28	1.28
4)	2.46	1.25	1.43	1.46	1.46	1.50	1.54	1.57	1.60	1.60	1.64	1.68
5)	2.6	1.13	1.27	1.33	1.40	1.40	1.43	1.47	1.47	1.47	1.50	1.53
6)	2.55	1.10	1.21	1.28	1.28	1.31	1.34	1.34	1.34	1.37	1.45	1.45
7)	2.52	1.17	1.31	1.38	1.42	1.43	1.48	1.52	1.52	1.52	1.55	1.58
8)	2.67	1.09	1.14	1.19	1.24	1.29	1.29	1.29	1.29	1.33	1.38	1.43
9)	2.58	1.21	1.25	1.29	1.33	1.33	1.37	1.42	1.42	1.42	1.46	1.54
10)	3.0	1.18	1.35	1.41	1.47	1.53	1.59	1.59	1.59	1.59	1.59	1.59
11)	2.32	1.23	1.32	1.41	1.50	1.55	1.55	1.55	1.55	1.59	1.68	1.77
12)	2.44	1.37	1.50	1.56	1.62	1.62	1.62	1.62	1.62	1.62	1.75	1.87
13)	2.42	1.14	1.24	1.29	1.29,	1.33	1.33	1.33	1.38	1.38	1.38	1.43
14)	2.55	1.17	1.39	1.50	1.55	1.66	1.66	1.66	1.66	1.72	1.77	1.88

TABLE 7. Rehydration Ratio, R_H/R_{HD}, as a function of time; Batch #2

		1 sec	2 sec	3 sec	4 sec	5 sec	10 sec	15 sec	30 sec	1 min	2 min	3 min
1)	3.0	1.55	1.75	1.80	1.85	1.90	2.00	2.05	2.10	2.15	2.20	2.25
2)	2.88	1.64	1.88	2.00	2.12	2.20	2.28	2.32	2.48	2.48	2.48	2.48
3)	2.90	1.48	1.72	1.86	1.90	1.96	2.03	2.10	2.14	2.14	2.17	2.17
4)	2.82	1.78	2.09	2.22	2.30	2.48	2.48	2.48	2.48	2.61	2.61	2.61
5)	2.95	1.86	2.10	2.33	2.38	2.38	2.52	2.52	2.57	2.61	2.67	2.67
6)	2.90	1.90	2.10	2.25	2.30	2.30	2.30	2.30	2.35	2.40	2.45	2.45
7)	3.69	1.75	2.06	2.13	2.25	2.25	2.25	2.25	2.43	2.43	2.43	2.43
8)	2.80	1.75	1.95	2.10	2.20	2.25	2.25	2.25	2.40	2.40	2.45	2.50
9)	2.79	1.59	1.79	1.90	1.97	2.00	2.07	2.14	2.24	2.31	2.41	2.41
10)	2.84	1.65	1.88	2.00	2.08	2.15	2.27	2.31	2.31	2.35	2.40	2.40
11)	2.87	1.67	1.83	1.96	2.00	2.00	2.04	2.04	2.08	2.12	2.12	2.12
12)	3.06	1.75	2.125	2.19	2.31	2.37	2.37	2.43	2.56	2.56	2.56	2.56

TABLE 8. Rehydration Ratio, R_H/R_{HD} as a function of time, Batch #3

		1 sec	2 sec	3 sec	4 sec	5 sec	10 sec	15 sec	30 sec	1 min	2 min	3 min	
1)	2.88	1.61	1.67	1.83	1.83	1.89	1.94	2.0	2.0	2.05	2.16	2.28	
2)	2.83	1.55	1.72	1.83	1.83	1.94	2.0	2.05	2.11	2.22	2.22	2.22	2.27
3)	3.0	1.5	1.65	1.80	1.90	1.95	1.95	2.0	2.05	2.15	2.20	2.30	
4)	2.84	1.64	1.76	1.84	1.88	1.96	1.96	2.04	2.04	2.04	2.08	2.12	
5)	2.84	1.40	1.64	1.76	1.80	1.92	2.0	2.0	2.0	2.04	2.04	2.04	2.09
6)	2.75	1.62	1.83	1.91	1.96	2.0	2.04	2.04	2.08	2.12	2.12	2.12	
7)	3.0	1.75	2.0	2.10	2.15	2.25	2.35	2.35	2.35	2.35	2.35	2.35	
8)	3.1	1.75	1.95	2.10	2.15	2.20	2.25	2.35	2.40	2.45	2.5	2.5	2.37
9)	3.0	1.58	1.74	1.84	1.95	1.95	2.05	2.10	2.10	2.21	2.21	2.26	
10)	2.82	1.78	1.91	2.04	2.09	2.09	2.13	2.13	2.17	2.26	2.35	2.43	
11)	2.68	1.36	1.5	1.54	1.59	1.59	1.68	1.72	1.72	1.72	1.72	1.72	2.14
12)	2.93	1.62	1.79	1.93	1.96	2.03	2.03	2.07	2.14	2.14	2.21	2.28	

TABLE 9. Rehydration Ratio, R_H/R_{HD}, as a function of time; Batch #4

	1 sec	2 sec	3 sec	4 sec	5 sec	10 sec	15 sec	30 sec	1 min	2 min	3 min
1)	1.60	1.80	1.90	1.97	2.00	2.04	2.08	2.13	2.18	2.21	2.27
2)	1.65	1.83	1.94	2.01	2.07	2.12	2.14	2.18	2.21	2.23	2.26
3)	1.57	1.81	1.91	1.99	2.04	2.09	2.13	2.17	2.22	2.26	2.28
4)	1.73	1.88	1.97	2.03	2.08	2.13	2.16	2.19	2.22	2.23	2.26

TABLE 10. Rehydration Ratio, R_H/R_{HD}, as a function of time; batch #5

r = Fraction of Rehydration (Experimental - $\frac{M_w}{M_{w_x}}$) Batch #5

	Before Rehydr	1 sec	2 sec	3 sec	4 sec	5 sec	10 sec	15 sec	30 sec	1 min	2 min	3 min
1)	0.0	0.312	0.423	0.476	0.513	0.529	0.550	0.571	0.598	0.624	0.640	0.672
2)	0.0	0.344	0.439	0.497	0.534	0.567	0.593	0.604	0.624	0.641	0.651	0.667
3)	0.0	0.301	0.428	0.482	0.524	0.551	0.577	0.598	0.620	0.645	0.677	0.667
4)	0.0	0.387	0.466	0.512	0.546	0.572	0.599	0.614	0.631	0.645	0.651	0.668

TABLE 11. Fraction of Rehydration, $r = \frac{M_w}{M_{w_x}}$, as a function of time; Batch #5

R_H = Rehydration Number (Experimental - $\frac{M}{M_o}$) Batch #5

	Before Rehyd.	1 sec	2 sec	3 sec	4 sec	5 sec	10 sec	15 sec	30 sec	1 min	2 min	3 min
1)	0.346	0.553	0.622	0.656	0.681	0.694	0.704	0.718	0.738	0.754	0.763	0.783
2)	0.346	0.571	0.626	0.672	0.699	0.717	0.734	0.740	0.754	0.766	0.774	0.780
3)	0.346	0.546	0.627	0.663	0.688	0.708	0.726	0.746	0.752	0.764	0.779	0.790
4)	0.346	0.599	0.649	0.679	0.700	0.721	0.735	0.750	0.759	0.766	0.772	0.782

TABLE 12. Rehydration Number, M/M_o, as a function of time; Batch #5

THERMOCOUPLE TEMPERATURE (°C)

TIME	1000	1100	1200	1300	1400	1500	1600	1700	1800	1900	2000
TC# / POSITION											
10 / 1/4 cm	-18	-13	-13	-12	-10	-10	-9	-9	-7	-7	-6
15 / 1/2 cm	-18	-14	-14	-13	-11	-11	-10	-8	-8	-8	-7
12 / 3/4 cm	-18	-15	-15	-14	-12	-12	-11	-9	-9	-9	-8
13 / 1 cm	-18	-16	-16	-15	-13	-13	-12	-10	-10	-10	-9

TURKEY SLICE

x	1-x	θ	$\frac{\theta}{1-x}$
1.0	0.0	0.0	0.0
0.9	0.1	1.6	16.0
0.8	0.2	3.3	16.5
0.7	0.3	5.1	17.0
0.6	0.4	7.0	17.5
0.5	0.5	9.0	18.0
0.4	0.6	11.1	18.5
0.3	0.7	13.3	19.0
0.2	0.8	16.4	20.9
0.1	0.9	21.6	24.0
0.0	1.0	30.0	25.0

Above taken from strip chart recorder plot

APPENDIX B
SAMPLE CALCULATIONS

Predicted Rehydration (capillary height h_1 – any direction)

Assume "effective sarcollemma diameter" is one quarter "actual sarcollemma diameter" –

i.e. $d = 0.0006$ cm

$$h_1^2 = \frac{d}{4} \frac{\gamma}{\mu} g\, t$$

$$r = \frac{h_1}{L_1}$$

$$t = \frac{4\, \mu\, L_1^2}{g\, \gamma\, d}$$

For $d = 0.0006$ cm

$\gamma = 70.0$ gm/sec^2

$\mu = 0.01$ gm/cm-sec

$L_1 = 2.2$ cm

t(sec)	h_1(cm)	r
1	1.05	0.477
2	1.50	0.682
3	1.80	0.819
4	2.10	0.95
4.6	2.20	1.00

Square root of ratio of surface tension over viscosity for water.

Temp °F	Ratio [Ref. 21] $\frac{\gamma}{\mu}$	Square root of of ratio $[\frac{\gamma}{\mu}]^{1/2}$
40	0.159	0.399
80	0.273	0.523
100	0.337	0.381
120	0.398	0.632
160	0.527	0.726
180	0.587	0.766
212	0.680	0.826

APPENDIX C

In order to prevent "over-drying" it is necessary to have an end-of-run indication. It is desirable that this end-of-run indication be reliable, inexpensive and easily recordable. One parameter which can provide end-of-run indication is specimen weight, since the evolution of freeze-drying is completed when there is no further removal of water vapor from the specimen. An analytic balance is not satisfactory because it requires continuous local operation. A Mettler Scale is prohibitive because of its high cost. In fact, a weight-measuring device is not necessary. All that is needed is an indication of the change in weight. The weight-change-indication-device (WCID) was designed to fulfill this requirement.

Physically the WCID is put together on a chemistry stand 30 inches high. At the top of the stand is clamped a cross-bar from which hangs a specimen tray. The specimen tray is suspended by a spring which allows up and down movement of the specimen tray as the specimen weight changes. The spring is, of course, linear for the range of the specimen weight. At the bottom of the specimen tray is attached the movable core of a linear core transducer. The static outer cylinder of the transducer is clamped to the bottom of the chemistry stand. Excitation to the linear core transducer is provided by an audio oscillator. The output of the transducer is fed to a voltmeter and a trace

recorder. The WCID is extremely versatile due to two of its features. By changing the spring, the WCID can be adapted to handle extremes of specimen weights. Because of this feature the WCID is usable over a greater range of weights than either an analytic balance or a Mettler Scale. The second feature is the facility for adjusting the gain of the amplifier and the null position of the movable core transformer. This permits the setting of a wide range of sensitivity.

Figure 20 is an illustration of the WCID.

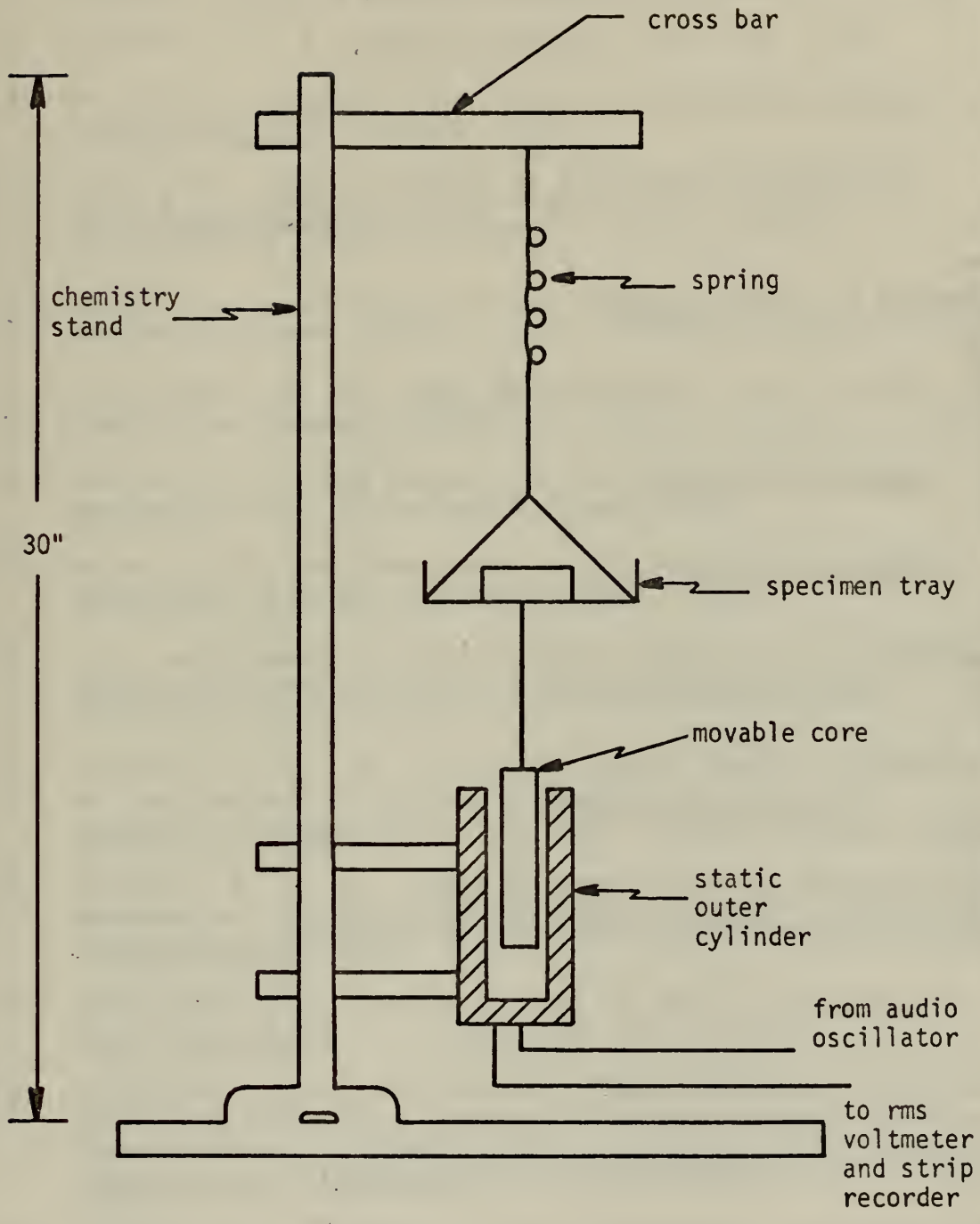

Figure 20. Weight change indicator device

BIBLIOGRAPHY

1. King, C. Judson, Freeze-Drying of Foods, CRC Press, 1971.

2. Flosdorf, K. W., Freeze-Drying, Reinhold, 1949.

3. Rey Louis, Aspects Theoriques et Industrias de la Lyophilisation, Hermann, 1964.

4. Noyes, R., Freeze Drying of Food and Biologicals, Food Processing Review #1, Noyes Development Corporation, 1968.

5. Cotson, S., and Smith, D.B., Freeze-Drying of Foodstuffs, Columbine Press, 1962.

6. Van Arsdel, W. B., Food Dehydration, Vol. I, AVI Publishing Company, 1964.

7. Harper, I. C. and Tappel, A. L., Advances in Food Research, Vol. 7, Academic Press, 1957.

8. Burke, R. F. and Decareau, R. U., Advances in Food Research, Vol. 13, Academic Press, 1957.

9. U.S. Department of Agriculture, List No. 77, Freeze-Drying of Foods, a List of Selected References, Corridan, G. A., 1964.

10. Fulford, G. D., "A Survey of Recent Soviet Research on the Drying of Solids", Canadian Journal of Chemical Engineering, v. 47, p. 378-391, August 1969.

11. Meffert, H. F. T., "Heat Transmission in Freeze-Drying Materials," Proceedings XI International Congress on Refrigeration, 1963.

12. Bralsford, R., "Freeze-Drying of Beef," Journal of Food Technology, v. 2, p. 339, 353, 1967.

13. Brajnikov, A. M. and others, "Heat and Mass Transfer in Porous Materials During the Freeze-Drying Process Under Vacuum," International Institute of Refrigeration, Commission X, Lausanne, p. 11-17, 1969.

14. Luikov, A. V., "Heat and Mass Transfer in Freeze-Drying at High Vacuum," International Institute of Refrigeration, Commission X, Lausanne, p. 143-154, 1969.

15. Hardin, T. C., Ph. D. Thesis, Georgia Institute of Technology, Atlanta, 1965.

16. Margaritis, A. and King, C. J., Factors Governing Terminal Rates of Freeze-Drying of Poultry-Meats. Paper presented at A.I.Ch.E., Portland, Oregon, 1969.

17. Beke, G., "The Effect of the Sublimation Temperature on the Rate of the Freeze-Drying Process and Upon the Volumetric Change in Meat Muscle Tissue," Proceedings of the XII International Congress of Refrigeration, v. 3, 1969.

18. Clark, J. P., Ph. D. Thesis, University of California, Berkeley, 1968.

19. Hatcher, J. D., Ph. D. Thesis, Georgia Institute of Technology, Atlanta, 1964.

20. Spiess, W. E. L. and others, "The Influence of the Structure on the Mass Transfer in Freeze-Drying," International Institute of Refrigeration Commission X, Lausanne, p. 155-166, 1969.

21. Sandall, O. C., Interactions Between Heat and Mass Transfer in Freeze-Drying, Ph. D. Thesis, University of California, Berkeley, 1966.

22. Sandall, O. C.; King, C. J.; and Wilke, C. R.; "The Relationship Between Transport Properties and Rate of Freeze-Drying of Poultry Meat," A.I.Ch.E. Journal, v. 13, p. 428-438, May, 1967.

23. Gunn, R. D., Ph. D. Thesis, University of California, Berkeley, 1967.

24. King. C. J., Lam, W. K. and Sandall, O. C., "Physical Properties Important for Freeze-Drying Poultry Meat," Food Technology, Vol. 22, October 1968.

25. Goldblith, S. A., Exploration in Future Food Processing Techniques, MIT Press, Cambridge, Mass., 1963.

26. Chichester, C. O., Mrak, W. M. and Stewart, G. F., Advances in Food Research, Vol. 10, Academic Press, 1960.

27. Maximow, A. A. and Bloom, W., A Textbook of Histology, W. B. Saunders, Philadelphia, Pennsylvania, 1945.

28. Koonz, C. H. and J. M. Ramsbottom, "A Method for Studying the Histological Structure of Frozen Products. I. Poultry," Food Research, Vol. IV, p. 117, 1939.

29. Moore, W. J., Physical Chemistry, Prentice-Hall, Inc., 1962.

30. Barron, C. M., Physical Chemistry, McGraw-Hill, 1966.

31. Streeter, V. L., Fluid Mechanics, McGraw-Hill, 1971.

INITIAL DISTRIBUTION LIST

		No. Copies
1.	Library, Code 0212 Naval Postgraduate School Monterey, California 93940	2
2.	Defense Documentation Center Cameron Station Alexandria, Virginia 22314	2
3.	Professor Paul F. Pucci Code 59Pc Department of Mechanical Engineering Naval Postgraduate School Monterey, California 93940	2
4.	Chairman, Department of Mechanical Engineering Code 59 Naval Postgraduate School Monterey, California 93940	1
5.	LCDR Leonard Anderson Hamilton 801 Arbor Place Monterey, California 93940	6

Security Classification

DOCUMENT CONTROL DATA - R & D

(Security classification of title, body of abstract and indexing annotation must be entered when the overall report is classified)

1. ORIGINATING ACTIVITY (Corporate author)	2a. REPORT SECURITY CLASSIFICATION
Naval Postgraduate School Monterey, California 93940	Unclassified
	2b. GROUP

3. REPORT TITLE

Freeze-Drying and Rehydration

4. DESCRIPTIVE NOTES (Type of report and inclusive dates)

Master's Thesis; June 1973

5. AUTHOR(S) (First name, middle initial, last name)

Leonard Anderson Hamilton

6. REPORT DATE	7a. TOTAL NO. OF PAGES	7b. NO. OF REFS
June 1973	96	31

8a. CONTRACT OR GRANT NO.	9a. ORIGINATOR'S REPORT NUMBER(S)
b. PROJECT NO.	
c.	9b. OTHER REPORT NO(S) (Any other numbers that may be assigned this report)
d.	

10. DISTRIBUTION STATEMENT

Approved for public release; distribution unlimited.

11. SUPPLEMENTARY NOTES	12. SPONSORING MILITARY ACTIVITY
	Naval Postgraduate School Monterey, California 93940

13. ABSTRACT

Experimental results using roast turkey meat were obtained substantiating the uniformly retreating ice front model used in freeze-drying.

A one dimensional model for rehydration was developed, based on flow in capillary tubes. Experimental results using roast turkey meat compared favorably with model predictions for an effective capillary diameter of 0.0010 cm. The results indicate a rapid rehydration following the model behavior predicted, followed by a much slower rate of rehydration. Maximum rehydration of the samples tested was to approximately two thirds of the original water content, eighty percent of which occurred during the first, rapid rehydration period.

The experiments also confirmed the model prediction of increased rehydration with increasing temperature.

DD FORM 1 NOV 68 1473 (PAGE 1)

S/N 0101-807-6811

Security Classification

A-31408

KEY WORDS	LINK A		LINK B		LINK C	
	ROLE	WT	ROLE	WT	ROLE	WT
freeze-drying						
rehydration						
theory of freeze-drying						
theory of rehydration						
freeze-drying model						
rehydration model						
diffuse frozen front						
discrete frozen front						
sublimation front						
capillarity						
effective capillary diameter						
freeze-drying plant						
weight change indication device						

Thesis 145197
H16375 Hamilton
c.1 Freeze-drying and re-
hydration.